Induced Second-Class-Current Effects in Hyperon Beta Decay*

P. L. Pritchett and N. G. Deshpande†
Department of Physics, Northwestern University, Evanston, Illinois 60201
(Received 23 March 1973)

Within the framework of the Cabibbo theory we investigate the role played by SU(3)-symmetry breaking in generating a pseudotensor form factor $g_2(q^2)$ in the hadronic matrix element for hyperon beta decay. Such an estimate is necessary before one can infer the existence of second-class currents from the experimental observation of this term. $g_2(q^2)$ is assumed to obey an unsubtracted dispersion relation, and the contributions to the dispersion integral from the lowest-mass two-body intermediate states (the vector–pseudoscalar-meson states) are studied. The imaginary part of the form factor is computed from the triangle graph in which single-baryon exchange is retained as the scattering mechanism. The violation of unitarity by this mechanism above the $B\bar{B}$ annihilation threshold provides a natural cutoff in the dispersion integral. Known mass breakings and estimates of SU(3)-coupling breakings are used to determine values of $g_2(0)$ for all the $\Delta S = 1$ beta decays of the $J^P = \frac{1}{2}^+$ hyperons and for the $\Sigma^\pm \to \Lambda$ beta decays. The corrections to this calculation arising from higher-mass states (tensor–pseudoscalar-meson and baryon-antibaryon) are found to be quite small. The effects of axial-vector–meson resonances on the vector-pseudoscalar calculation are also examined. The computed value of $g_2(0)$ for $\Lambda \to p$ beta decay is more than an order of magnitude smaller than the value suggested by some experiments. The implications of this result for the existence of second-class currents are discussed. The $\Sigma^\pm \to \Lambda$ decays are predicted to have the largest induced value of $g_2(0)$. The utility of these decays in distinguishing between real second-class effects and those induced by SU(3) breaking is stressed.

I. INTRODUCTION

The Cabibbo theory[1] has proved to be quite successful in describing semileptonic interactions. Thus the simplest version of this theory, which maintains manifest SU(3) symmetry, provides a very good over-all fit to the data on the leptonic decays of baryons.[2] Recent experiments on the beta decay of polarized Λ hyperons,[3-6] however, have produced conflicting evidence regarding the possible existence of large deviations from this simple Cabibbo theory. Since it is known that SU(3) is not an exact symmetry, the occurrence of some discrepancy is not unexpected. The interesting question rather is whether the discrepancy can be understood on the basis of SU(3) breaking or whether a drastic revision of the Cabibbo theory is required. In particular, some of the polarized Λ experiments suggest the presence of a large pseudotensor term in the matrix element of the axial-vector current.[7] Such a term could be caused by SU(3)-breaking effects in the Cabibbo theory, or it could reflect the existence of a new interaction in the weak Hamiltonian involving second-class currents. Since the second alternative would necessitate a major revision in our understanding of weak interactions, it is clearly of great importance to determine whether the suggested experimental effect can be explained by the first possibility. At present no quantitative estimate exists of how large a pseudotensor term could be induced by SU(3) breaking. In the present paper we undertake to make such an estimate.[8]

The Cabibbo Hamiltonian for semileptonic interactions is of the form[9]

$$\mathcal{H}_W = -(G/\sqrt{2})(J_\mu^{(+)} l_\mu^{(-)} + J_\mu^{(-)} l_\mu^{(+)}). \tag{1.1}$$

The leptonic current is

$$l_\lambda^{(-)} = i\bar{\Psi}_e \gamma_\lambda (1+\gamma_5)\Psi_{\nu_e} + i\bar{\Psi}_\mu \gamma_\lambda (1+\gamma_5)\Psi_{\nu_\mu}, \tag{1.2}$$

while the matrix element of the hadronic current between baryon states is given by

$$\langle B_2(p_2)|J_\mu^{(+)}(0)|B_1(p_1)\rangle = i(m_1 m_2/E_1 E_2 \Omega^2)^{1/2} \times \bar{u}_2(p_2)\Gamma_\mu u_1(p_1), \tag{1.3}$$

where[10]

$$\Gamma_\mu = f_1(q^2)\gamma_\mu + \frac{f_2(q^2)\sigma_{\mu\nu}q_\nu}{(m_1+m_2)} + i\frac{f_3(q^2)q_\mu}{(m_1+m_2)} + g_1(q^2)\gamma_\mu\gamma_5 + \frac{g_2(q^2)\sigma_{\mu\nu}q_\nu\gamma_5}{(m_1+m_2)} + i\frac{g_3(q^2)q_\mu\gamma_5}{(m_1+m_2)}, \tag{1.4}$$

and $q \equiv p_1 - p_2$. Time-reversal invariance implies

that the f_i and g_i are real. Weinberg[11] has classified currents as "first class" or "second class" according to their transformation properties under G parity,

$$G = C\exp(-i\pi T_2). \tag{1.5}$$

First-class vector and axial-vector currents satisfy

$$\begin{aligned} G V_\mu^{(\mathrm{I})}(0) G^{-1} &= V_\mu^{(\mathrm{I})}(0), \\ G A_\mu^{(\mathrm{I})}(0) G^{-1} &= -A_\mu^{(\mathrm{I})}(0), \end{aligned} \tag{1.6}$$

while second-class currents satisfy

$$\begin{aligned} G V_\mu^{(\mathrm{II})}(0) G^{-1} &= -V_\mu^{(\mathrm{II})}(0), \\ G A_\mu^{(\mathrm{II})}(0) G^{-1} &= A_\mu^{(\mathrm{II})}(0). \end{aligned} \tag{1.7}$$

For the case of strangeness-changing currents, a similar classification can be made based on the behavior under the G' transformation,[12]

$$G' = C\exp(-i\pi V_2). \tag{1.8}$$

In the Cabibbo theory it is assumed that the hadronic currents appearing in the *Hamiltonian* (1.1) are of first class only. It then follows as a consequence of G parity that for transitions within an isotopic multiplet, such as $n \to p + e^- + \bar{\nu}_e$, the scalar term $f_3(q^2)$ and the pseudotensor term $g_2(q^2)$ in the *matrix element* of the current [cf. Eqs. (1.3) and (1.4)] vanish identically.[13] Similarly, for transitions within a V-spin multiplet, such as $\Sigma^- \to n + e^- + \bar{\nu}_e$, G' invariance ensures the vanishing of f_3 and g_2. For transitions involving more than one I-spin or V-spin multiplet, such as $\Sigma^- \to \Lambda + e^- + \bar{\nu}_e$ and $\Lambda \to p + e^- + \bar{\nu}_e$, SU(3) symmetry plus charge conjugation yield $f_3 = 0 = g_2$. When G, G', or SU(3) is broken, nonzero values of f_3 and g_2 can be induced by the symmetry-breaking interaction.[14] In contrast, if a second-class current is present in the Hamiltonian, then nonvanishing values of f_3 and g_2 appear in the matrix element even in the limit of exact SU(3).

The smallness of the electron mass renders f_3 essentially unobservable in electron decays. The relatively large momentum transfer available in $\Delta S = 1$ hyperon decays, however, makes detection of the pseudotensor term feasible. Of these decays, the most easily accessible experimentally are $\Lambda \to p + e^- + \bar{\nu}_e$ and $\Sigma^- \to n + e^- + \bar{\nu}_e$, and we shall concentrate on computing $g_2(0)$ for these two decays. The strangeness-conserving decays $\Sigma^- \to \Lambda + e^- + \bar{\nu}_e$ and $\Sigma^+ \to \Lambda + e^+ + \nu_e$ also involve relatively large momenta. For these decays G parity requires that the magnitudes of the matrix elements be equal.[15] SU(3) breaking can then induce nonzero values of g_2 such that g_2/g_1 is the same for both decays. On the other hand, the addition of a second-class current to the Hamiltonian would lead [in the limit of exact SU(3)] to equal but opposite values of g_2/g_1 for the two decays. For future reference we summarize in Table I the Cabibbo predictions[2] for the $\Lambda \to p$, $\Sigma^- \to n$, and $\Sigma^\pm \to \Lambda$ beta decays.

Our calculation of the induced pseudotensor form factor $g_2(q^2)$ will be based on dispersion relations. We assume that $g_2(q^2)$ satisfies an unsubtracted dispersion relation:

$$g_2(q^2) = \frac{1}{\pi}\int_{\sigma_2}^{\infty} \frac{\mathrm{Im} g_2(-\sigma^2)\, d\sigma^2}{\sigma^2 + q^2 - i\epsilon}\,. \tag{1.9}$$

Furthermore, we assume that the dispersion integral is dominated by the lowest-mass intermediate states. The motivation behind these assumptions is discussed in Sec. II. There the dispersion approach to the calculation of form factors is illustrated by the case of the anomalous isovector magnetic moment of the nucleon. The evaluation of the two-pion contribution to the anomalous-moment form factor is reviewed, and the new complications that arise in the pseudotensor case are indicated. The lowest-mass two-body states that contribute to the integral in Eq. (1.9) consist of a vector and a pseudoscalar meson. Section III is devoted to the evaluation of the triangle graph for these states in which only single-baryon exchange is retained as a scattering mechanism. The SU(3)-symmetric vertex functions are determined, $\mathrm{Im} g_2(-\sigma^2)$ is computed, and questions regarding the convergence of the dispersion integral are investigated. Many of the details of the analysis are contained in the Appendixes. Numerical results for $g_2(0)$ are presented for the beta decays $\Lambda \to p$, $\Sigma^- \to n$, $\Sigma^\pm \to \Lambda$, $\Xi^- \to \Lambda$, and $\Xi^0 \to \Sigma^+$. The effects of breaking of SU(3) couplings and the existence of axial-vector resonances on these results are also considered. In Sec. IV higher-mass states are investigated, in particular the tensor–pseudoscalar-meson and baryon-antibaryon states. Section V summarizes the results obtained for the

TABLE I. Predictions of the Cabibbo model for various hyperon beta decays.

Beta decay	$f_1(0)$	$f_2(0)/f_1(0)$	$g_1(0)/f_1(0)$
$\Lambda \to p$	−0.29	1.79	0.72
$\Sigma^- \to n$	−0.24	−2.03	−0.34
$\Sigma^\pm \to \Lambda$	0	3.62 [a]	∓ 0.63 [b]

[a] $f_2(0)/g_1(0)$.
[b] $g_1(0)$ only.

induced pseudotensor term and discusses their experimental implications.

II. DISPERSION CALCULATION OF FORM FACTORS

Our approach to computing the pseudotensor form factor reflects the long experience gained from calculations of the anomalous magnetic moments of the nucleon. The early history of the attempts to explain these anomalous moments in terms of meson theory has been summarized by Bethe and de Hoffmann.[16] The most successful method developed has been the use of dispersion relations.[17,18] Before describing the dispersion approach, however, it is useful to recall the results of perturbation theory. To second order in the pion-nucleon coupling constant there are two diagrams (see Fig. 1) that contribute to the anomalous magnetic moment. The contributions to the proton and neutron moments from these graphs have the form

$$\lambda_p = B_a - \tfrac{1}{2}B_b, \qquad \lambda_n = -B_a - B_b, \tag{2.1}$$

where B_a and B_b are constants computed from the two graphs. Thus the pion diagram 1(a) contributes only to the isovector moment ($\lambda^V \equiv \frac{1}{2}\lambda^p - \frac{1}{2}\lambda^n$), while the nucleon diagram 1(b) contributes to both the isovector and isoscalar ($\lambda^S \equiv \frac{1}{2}\lambda^p + \frac{1}{2}\lambda^n$) moments. Assuming the usual pseudoscalar coupling with $g_{\pi NN}^2/4\pi = 14.6$, one finds (in units of nucleon magnetons) $B_a = 1.62$ and $B_b = 2.19$.[19] One thus obtains $\lambda_p = 0.52$ and $\lambda_n = -3.81$ to be compared with the experimental values $\lambda_p = 1.79$ and $\lambda_n = -1.91$. Both signs are correct, but the magnitudes are wrong by factors of three and two. Calculation of the fourth-order diagrams[20] does not improve the agreement. In terms of λ^V and λ^S the perturbation results are $\lambda^V = B_a + \frac{1}{4}B_b = 2.17$ and $\lambda^S = -\frac{3}{4}B_b = -1.64$. The experimental values are $\lambda^V = 1.85$ and $\lambda^S = -0.06$. Note that the pion diagram by itself gives a quite good result ($\lambda^V = 1.62$) for the isovector moment, while the very poor result for the isoscalar moment is due entirely to the very large contribution from the nucleon diagram. It is thus tempting to argue that the nucleon contribution should be suppressed by some mechanism. Dispersion theory, to which we now turn, introduces this suppression in a natural manner.

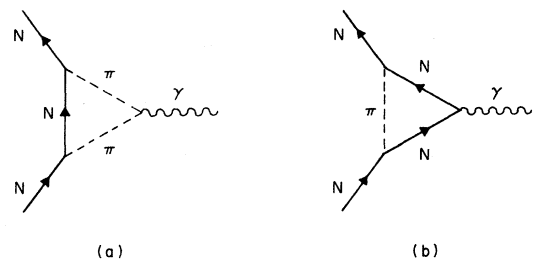

FIG. 1. Feynman diagrams to order $g_{\pi NN}^2$ that contribute to the anomalous magnetic moments of the nucleon.

The nucleon electromagnetic vertex can be expressed in terms of two couplings, a charge term $F_1(q^2)\gamma_\mu$ and a magnetic-moment term $F_2(q^2)\sigma_{\mu\nu}q_\nu/(2m)$. The form factors $F_{1,2}$ are assumed to satisfy dispersion relations in the momentum-transfer variable q^2. For $F_2(q^2)$ the equation is taken to be unsubtracted:

$$F_2^{V,S}(q^2) = \frac{1}{\pi}\int \frac{\mathrm{Im}F_2^{V,S}(-\sigma^2)d\sigma^2}{\sigma^2 + q^2 - i\epsilon}\ ; \tag{2.2}$$

for $F_1(q^2)$ a once-subtracted equation is normally assumed where the subtraction constant is known from the value of the electric charge. The absorptive parts of the form factors can be expressed in terms of a sum over all the intermediate states that can be reached from the electromagnetic current and lead to a nucleon-antinucleon pair. The lowest-mass state that contributes to this sum is the two-pion state, and it contributes only to the isovector form factors. Higher-mass states include many pions, $K\bar{K}$, nucleon-antinucleon, etc. Now a particular state in the sum contributes only with a threshold equal to the square of the total rest mass of the state. One might thus expect that at low q^2 the contributions to the dispersion integral (2.2) of the high-mass states would be small compared to those of the low-mass states. In particular, one expects the isovector form factors to be dominated by the two-pion state.

The simplest possible treatment of the two-pion state is to describe the annihilation $N\bar{N} \to \pi\pi$ by the Born term and to neglect the electromagnetic structure of the pion. With these approximations, the dispersion relation (2.2) yields precisely the same results as those obtained in lowest-order perturbation theory. As we have noted above, this result for the anomalous isovector magnetic moment is quite good. Federbush, Goldberger, and Treiman,[18] however, concluded that these approximations are not justified. When the dispersion variable $\sigma^2 > 4m^2$, $N\bar{N}$ annihilation into two pions becomes a physical process, and the amplitude is then bounded by unitarity. Use of the Born approximation for the annihilation amplitude leads to a severe violation of unitarity in this region. The consequence of this violation is that the contribution to λ^V from the region $\sigma^2 > 4m^2$ in Eq. (2.2) is much larger [$\lambda^V(\sigma^2 > 4m^2) = 0.77$]

than the maximum value permitted by unitarity (0.2). The region $\sigma^2 < 4m^2$, where use of the Born approximation may be justified, contributes only 0.85 to the anomalous moment. Thus the good agreement between the perturbation result and experiment must be regarded as fortuitous. Federbush *et al.*[18] attempted to estimate the rescattering corrections by including $N^*(1232)$ exchange in addition to nucleon exchange. They found that the N^* contribution was very large. In fact, the contribution from the region $\sigma^2 < 4m^2$ was 1.00. If this is added to the Born contribution of 0.85, then impressive agreement with experiment is obtained. The evaluation of the N^* exchange, however, involved the use of a Legendre polynomial expansion outside its region of convergence, and so (as Federbush *et al.* emphasized) the rescattering correction was probably overestimated. Indeed, subsequent work has indicated that the correction from N^* exchange is small.[21] It thus appears that the rescattering corrections are not large enough to explain the anomalous moment.

The effect of the pion form factor was also investigated by Federbush *et al.*[18]. They used a scattering-length approximation for the pion phase shift with a length $\sim 1/m$, which is characteristic of a nucleon pair state. The resulting pion form factor did not greatly alter the results for the anomalous moment. It was subsequently pointed out by Frazer and Fulco,[21] however, that the assumption of a resonance in the $J=1$, $T=1$ state of the pion-pion system could bring the dispersion calculation of both the anomalous isovector moment and the isovector magnetic radius (and perhaps the isovector charge radius as well) into agreement with experiment. The resonance was predicted to have a mass of ~500 MeV and a width of ~100 MeV. From their investigation of partial-wave dispersion relations for the process $\pi + \pi \to N + \bar{N}$,[22] they found that to a good approximation the effect of the resonance appears simply as a multiplicative factor in the dispersion integral. Thus

$$\mathrm{Im}F_2^V(-\sigma^2) \approx |F_\pi(-\sigma^2)|^2 [\mathrm{Im}F_2^V(-\sigma^2)]_0, \qquad (2.3)$$

where $[\mathrm{Im}F_2^V(-\sigma^2)]_0$ is the spectral function calculated with pion-pion scattering neglected. The pion form factor thus leads to an enhancement of the spectral function in the vicinity of the resonance.

The subsequent discovery of the ρ meson[23] appeared to be a striking confirmation of the Frazer-Fulco prediction. One problem does remain, however, inasmuch as the experimental ρ mass ($\approx$770 MeV) is considerably larger than the predicted value. The question is whether this higher-mass resonance still produces a nucleon form factor consistent with experiment. For example, if in the evaluation of the nucleon exchange contribution one uses the approximation (2.3) together with the *experimental* pion form factor,[24] then one finds $\lambda^V \approx 5$, which is much too big. It appears that a better treatment of the $N\bar{N} \to \pi\pi$ amplitude than that used by Frazer and Fulco, e.g., the use of a two-pole rather than a one-pole effective-range formula[25] or the introduction of Regge-type asymptotic behavior for the nucleon pole and 3-3 resonance states,[26] together with the experimental parameters of the ρ does lead to a successful description of the low-q^2 behavior of the nucleon form factors.

Motivated by the success of the dispersion calculation of the anomalous moment, we shall employ a similar approach in the present investigation of the induced pseudotensor form factor $g_2(q^2)$. Thus our basic assumptions are that $g_2(q^2)$ satisfies an unsubtracted dispersion relation, Eq. (1.9), and that the dispersion integral is dominated by the lowest-mass intermediate states. The lowest-mass two-body states consist of a vector and a pseudoscalar meson. Again, the simplest possible treatment of these states is to describe the annihilation $B_1 + \bar{B}_2 \to V + M$ by the Born terms and to assume a point coupling of the weak current to the mesons. We then have to consider the triangle diagrams shown in Fig. 2. The presence in these graphs of a vector-meson propagator obtained from a nonrenormalizable theory leads to several difficulties not present in the anomalous moment case. First, if one evaluates $g_2(q^2)$ from the graphs in Fig. 2 treating them either as Feynman diagrams or using them to evaluate the discontinuity in the dispersion integral, the result is logarithmically divergent. It is thus necessary to introduce a cutoff in the calculation. Since single-baryon exchange in $B\bar{B} \to VM$ annihilation violates unitarity, it is natural to choose the cutoff where this violation

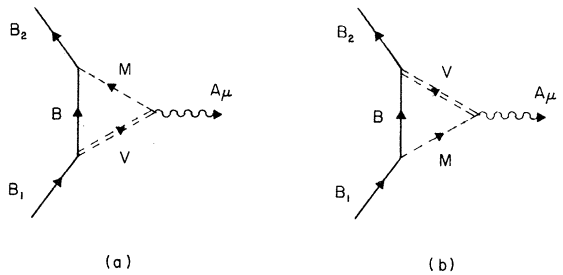

FIG. 2. Feynman diagrams used in the calculation of the induced pseudotensor term in the decay $B_1 \to B_2 + l^- + \bar{\nu}_l$.

first occurs, i.e., near threshold. Since this divergence occurs only in a numerically unimportant part of the coupling of the weak current to the mesons, the variation of the logarithmic term with cutoff is in fact insignificant compared with the dominant (finite) contribution to $g_2(q^2)$. A second difficulty is that if one computes this finite part from the unsubtracted dispersion relation (1.9) with the discontinuity obtained from the diagrams of Fig. 2, then the result differs from that given by the Feynman evaluation of these graphs. (Recall that in the anomalous moment case the two procedures gave the same results.) The reason for this is that the triangle diagram by itself does not satisfy an *unsubtracted* dispersion relation. Thus, the diagram contains terms that approach constants as $|q^2| \to \infty$. But the assumption of an unsubtracted dispersion relation is essential to our approach since we have no way of determining a subtraction constant. The question then is whether these poorly behaved terms should be included in the evaluation of the discontinuity from the triangle graph. (In a renormalizable theory such terms, of course, would never appear.) Fortunately, it turns out that these terms are of secondary importance, and so the results for $g_2(q^2)$ do not depend strongly on whether they are included or not.

Judging by the anomalous moment calculation, one should go beyond this simple treatment of the meson state and include the effect of axial resonances (A_1 and K_A) and corrections to the Born description of the annihilation amplitude. While we shall make some estimates of the resonance contribution, there is in the present case a new effect, namely, the breaking of SU(3) coupling constants, which appears to be a major unknown factor in the calculation. Until one can do better than make very rough estimates of the coupling breakings, it would not appear to be worthwhile to undertake a more complete dispersion calculation of the induced pseudotensor form factor.

III. MESON TRIANGLE GRAPH

A. Vertex Functions

The evaluation of the meson triangle graphs in Fig. 2 requires the determination of three vertex functions. With one exception to be discussed below, these functions initially are assumed to be SU(3)-symmetric. The induced pseudotensor term then arises solely from the mass breakings of the physical particles. Later, the effect of SU(3) breaking of the coupling constants will also be considered.

The pseudoscalar-meson–baryon couplings are taken to be

$$\mathcal{L}_{\bar{B}BM} = 2ig_{\pi NN}[(1-\alpha_M)if_{ijk} + \alpha_M d_{ijk}]\bar{B}^i\gamma_5 B^j M^k, \tag{3.1}$$

where $g_{\pi NN}{}^2/4\pi = 14.6$ and $\alpha_M \cong 0.62$ (corresponding to the ratio $F/D = 0.6$).

The vector-meson–baryon Lagrangian is assumed to be

$$\begin{aligned}\mathcal{L}_{\bar{B}BV} = {} & iG_1(if_{ijk})\bar{B}^i\gamma_\mu B^j V_\mu^k \\ & + iG_2[(1-\alpha_V)if_{ijk} + \alpha_V d_{ijk}] \\ & \times \bar{B}^i\sigma_{\mu\nu}B^j(\tfrac{1}{2}i)[\partial_\nu V_\mu^k - \partial_\mu V_\nu^k]/(m_i + m_j).\end{aligned} \tag{3.2}$$

Note that it is the dimensionless coupling G_2 that is assumed to be SU(3)-invariant.[27] This choice is motivated by the observation that SU(3) symmetry for the baryon magnetic moments appears to hold better when the moments are expressed in particle magnetons rather than in nucleon magnetons. The breaking of SU(3) in $\mathcal{L}_{\bar{B}BV}$, however, is due only to mass breaking of the baryons. The coupling constants in (3.2) are determined through the principle of vector-meson dominance. One assumes that the matrix elements of the electromagnetic current between arbitrary states are well represented by the sum of the vector-meson contributions,

$$\begin{aligned}\langle B_2|J_\mu^{\rm em}(0)|B_1\rangle = {} & \sum_V \frac{1}{2\gamma_V}\ \frac{\mu_V{}^2}{W_V(q^2)+q^2} \\ & \times \langle B_2|J_\mu^V(0)|B_1\rangle .\end{aligned} \tag{3.3}$$

The matrix element $\langle B_2|J_\mu^V(0)|B_1\rangle$ describes the interaction of an off-mass-shell vector meson with mass $-q^2$, while $W_V(q^2)+q^2$ is the inverse vector-meson propagator. The coupling constants γ_V are assumed to be independent of q^2, at least in the region $-\mu_V{}^2 \leq q^2 \leq 0$. For the case where B_1 and B_2 are spin-$\frac{1}{2}$ baryons, the matrix element of $J_\mu^{\rm em}$ has the general form

$$\langle B_2(p_2)|J_\mu^{\rm em}(0)|B_1(p_1)\rangle = i(m_1 m_2/E_1E_2\Omega^2)^{1/2}\bar{u}_2(p_2)[F_1^{\rm em}(q^2)\gamma_\mu + F_2^{\rm em}(q^2)\sigma_{\mu\nu}q_\nu/(m_1+m_2)]u_1(p_1), \tag{3.4}$$

where $q = p_1 - p_2$. By considering the isovector part of $J_\mu^{\rm em}$ between nucleon states at $q^2 = 0$, one finds from Eqs. (3.2)–(3.4)

$$\begin{aligned} G_1 &= 2(2\gamma_\rho)[W_\rho(0)/\mu_\rho{}^2]F_1^V(0) \\ &= 2\hat{\gamma}_\rho, \\ G_2 &= 2(2\gamma_\rho)[W_\rho(0)/\mu_\rho{}^2]F_2^V(0) \\ &= 4\hat{\gamma}_\rho\lambda^V, \end{aligned} \tag{3.5}$$

where we have defined $\hat{\gamma}_\rho \equiv \gamma_\rho W_\rho(0)/\mu_\rho{}^2$ and have used the results $F_1^V(0) = \frac{1}{2}$ and $F_2^V(0) = \lambda^V = 1.853$. From the Orsay storage-ring experiments[24] one finds

$$\hat{\gamma}_\rho{}^2/\pi = 2.54 \pm 0.23. \tag{3.6}$$

As discussed in Appendix A, we take $\hat{\gamma}_\rho$ to be positive. From the anomalous isoscalar magnetic moment of the nucleon, one then finds

$$\alpha_V = 0.774. \tag{3.7}$$

The matrix element of the axial-vector current between vector- and pseudoscalar-meson states can be determined using partial conservation of axial-vector current (PCAC) and current algebra. Since this matrix element is sensitive to the momenta involved, it is necessary to use hard-pion techniques.[28,29] Appendix A contains a detailed discussion of this axial-vector vertex. The principal result is the following expression for the vertex:

$$\begin{aligned} &(4\omega_M\omega_V\Omega^2)^{1/2}\langle M^k(k)|\sin\theta_C A_\mu^{(\Delta S=1)i}(0)|V^j(p)\rangle \\ &\quad = \sin\theta_C f_{ijk}[\epsilon_\mu F_1(q^2) + p_\mu(\epsilon\cdot q)F_2(q^2) \\ &\qquad + q_\mu(\epsilon\cdot q)F_3(q^2)], \end{aligned} \tag{3.8}$$

where $q \equiv p - k$, $\theta_C \cong 0.24$, $F_1(0) \cong 1.0$ GeV, and $F_2(0) \cong -0.4$ GeV^{-1}. The term F_3 does not contribute to the induced pseudotensor form factor. Note that it is not possible for a singlet meson to couple to the axial-vector current. Couplings such as $\omega_1 KA$ and $K^*\eta' A$ would constitute direct second-class axial-vector couplings and would produce a pseudotensor term that does not vanish in the SU(3) limit.[30,31] Thus we shall treat ϕ and η as the unmixed $Y = T = O$ member of an octet. For μ_η we shall use the physical mass, while for μ_ϕ we shall take the value from the Gell-Mann–Okubo mass formula in inverse mass squared,[32]

$$3/\mu_\phi{}^2 = 4/\mu_{K^*}{}^2 - 1/\mu_\rho{}^2 . \tag{3.9}$$

This yields $\mu_\phi = 952$ MeV. Use of mass squared would have given $\mu_\phi = 932$ MeV. The difference between these values is not significant for our results. The explicit meson states that couple to the (strangeness-changing) axial current are thus $K^*\pi$, $K^*\eta$, ρK, and ϕK.

For the $\Sigma^\pm \to \Lambda$ decays we need the matrix element of $A_\mu^{(\Delta S=0)}$ between meson states. The general form of this matrix element is the same as that in Eq. (3.8) but with $\sin\theta_C$ replaced by $\cos\theta_C$. As discussed in Appendix A, the numerical values for $F_1(0)$ and $F_2(0)$ are approximately the same as those for the $\Delta S = 1$ case. Thus the axial-vector vertex is very nearly SU(3)-symmetric.

B. Feynman Evaluation of $g_2(q^2)$

Having determined the vertex functions, one can proceed to the evaluation of the triangle graphs. The contribution from the diagram in Fig. 2(a) to the hadronic matrix element is then

$$\begin{aligned} &(m_1 m_2/E_1E_2\Omega^2)^{1/2}\bar{u}(p_2)g_{\pi NN}A_{VMB}^{1,2}(2\pi)^{-4}\int d^4k\,\gamma_5(ik\cdot\gamma + m)^{-1}[G_1\gamma_\nu + G_2\sigma_{\nu\lambda}(p_1 - k)_\lambda/(m_1 + m)] \\ &\quad \times \sum_{\rm pol}\epsilon_\nu[(p_2 - k)^2 + \mu_M{}^2]^{-1}[\epsilon_\mu F_1 + (\epsilon\cdot q)(p_1 - k)_\mu F_2 + (\epsilon\cdot q)q_\mu F_3][(p_1 - k)^2 + \mu_V{}^2]^{-1}u(p_1). \end{aligned} \tag{3.10}$$

All the SU(3) dependence has been absorbed into the term $A_{VMB}^{1,2}$. The expression for the diagram in Fig. 2(b) is quite similar. The vector-meson polarization sum is given by

$$\sum_{\rm pol}\epsilon_\mu(p)\epsilon_\nu(p) = \delta_{\mu\nu} + p_\mu p_\nu/\mu_V{}^2 . \tag{3.11}$$

The extraction of the pseudotensor term from Eq. (3.10) using standard techniques is straightforward but lengthy. The result has the general form [for Fig. 2(a)]

$$g_2^{(a)}(q^2) = -g_{\pi NN}A_{VMB}^{12}(16\pi^2)^{-1}2\left\{\int_0^\infty k^2dk^2\int_0^1 dx\int_0^x dy[H_1^{(a)}(x,y,q^2)+k^2H_2^{(a)}(x,y,q^2)]\right.$$
$$\times[k^2+q^2y(x-y)+\alpha^{(a)}(x)y+\beta^{(a)}(x)]^{-3}$$
$$\left.+\int_0^1 dx\int_0^x dy\,S^{(a)}(x,y,q^2)\right\}(m_1+m_2), \tag{3.12}$$

where

$$\alpha^{(a)}(x) = (m_1^2-m_2^2)(1-x)+\mu_M^2-\mu_V^2,$$
$$\beta^{(a)}(x) = m_1^2x^2+(\mu_V^2-m_1^2-m^2)x+m^2. \tag{3.13}$$

Explicit expressions for the functions $H_1^{(a)}(x,y,q^2)$, $H_2^{(a)}(x,y,q^2)$, and $S^{(a)}(x,y,q^2)$ are given in Appendix B. These expressions involve an expansion in terms of four products of coupling constants:

$$H_1^{(a)}(x,y,q^2) = \sum_{i,j=1}^{2} h_{1ij}^{(a)}(x,y,q^2)F_iG_j, \tag{3.14}$$

where F_i and G_j are the coupling constants appearing in Eqs. (3.8) and (3.2). Similar expressions hold for $H_2^{(a)}$ and $S^{(a)}$. The surface terms $S^{(a)}(x,y,q^2)$ in Eq. (3.12) arise from shifting variables in linearly (or worse) divergent integrals.[33] Note that the k^2 integration involving H_1 is convergent, while that for k^2H_2 is formally logarithmically divergent. The contribution from diagram 2(b), $g_2^{(b)}(q^2)$, has an expression identical to Eq. (3.12) but in terms of functions $H_1^{(b)}(x,y,q^2)$, $H_2^{(b)}(x,y,q^2)$, $S^{(b)}(x,y,q^2)$, $\alpha^{(b)}(x)$, and $\beta^{(b)}(x)$. $\alpha^{(b)}(x)$ and $\beta^{(b)}(x)$ are obtained from Eq. (3.13) by making the replacement $\mu_V \to \mu_M$. Explicit formulas for $H_1^{(b)}$, $H_2^{(b)}$, and $S^{(b)}$ are again to be found in Appendix B. In the following we shall refer to the calculation of $g_2(q^2)$ based on Eq. (3.12) for $g_2^{(a)}(q^2)$ and the analogous equation for $g_2^{(b)}(q^2)$ as the Feynman evaluation of the triangle graphs.

In the limit of exact SU(3) symmetry the induced pseudotensor term must vanish. Using the expressions in Appendix B, one can verify that when all the baryon masses are degenerate, all the vector masses are degenerate, and all the pseudoscalar masses are degenerate, $g_2(q^2)\equiv 0$. It should be noted, however, that this result is obtained only after summing over all the individual states contained in Fig. 2. The contribution from a single state need not vanish in the SU(3) limit. This property will be important when breaking of SU(3) couplings is considered.

It is useful to examine the convergence properties of Eq. (3.12) for $g_2(q^2)$ in more detail. [When it is not necessary to distinguish between Figs. 2(a) and 2(b), we shall drop the superscripts (a) and (b).] As noted above, the only possible divergence comes from the k^2H_2 term. From Appendix B we note that H_2 contains no F_1G_2 term. Thus the contribution proportional to F_1G_2 is finite. Furthermore, the F_1G_1 term has the form

$$h_{2F_1G_1}^{(a,b)} = \mp(1-\tfrac{3}{2}x)/2\mu_V^2. \tag{3.15}$$

If one cuts off the k^2 integral in Eq. (3.12) at $k^2=\Lambda^2$ and then integrates by parts, one finds that the coefficient of $\log\Lambda$ is zero. Thus as $\Lambda\to\infty$, the integral remains finite. Consequently, the contribution proportional to F_1G_1 (and thus the entire contribution proportional to F_1) is also finite. The F_2G_1 and F_2G_2 terms, however, are logarithmically divergent.

C. Dispersion Evaluation of $g_2(q^2)$

So far we have treated the triangle diagram simply as a Feynman graph. Now we want to compute $\mathrm{Im}g_2(-\sigma^2)$ and evaluate the dispersion integral (1.9). From Eq. (3.12) and Appendix B it is apparent that the discontinuity in q^2 arises solely from the denominator

$$D\equiv[k^2+q^2y(x-y)+\alpha(x)y+\beta(x)]^3 = y^3(x-y)^3(q^2+\gamma^2)^3, \tag{3.16}$$

where

$$\gamma^2\equiv[k^2+\alpha(x)y+\beta(x)]/y(x-y). \tag{3.17}$$

Note in particular that the surface terms $S^{(a,b)}$ do not contribute to the discontinuity. The discontinuity of the quantity $(q^2)^m/D$ is given by

$$\mathrm{Disc}[(q^2)^m/D] = \tfrac{1}{2}\pi(q^2)^m[d^2/d(q^2)^2]\delta(q^2+\gamma^2)\,. \tag{3.18}$$

Thus to compute $g_2(q^2)$ from the dispersion relation (1.9), we need to evaluate expressions of the form

$$R(q^2) = \frac{1}{2}\int_{\sigma_{\mathrm{th}}^2}^{\Lambda^2} \frac{d\sigma^2(-\sigma^2)^m}{\sigma^2+q^2} \int_0^\infty k^2dk^2\int_0^1 dx\int_0^x dy\, y^{-3}(x-y)^{-3}W(x,y,k^2)\delta''\big([k^2+\beta(x)+\alpha(x)y]/y(x-y)-\sigma^2\big). \tag{3.19}$$

We have introduced a cutoff $\sigma^2=\Lambda^2$ at the upper end of the dispersion integral in order to investigate convergence questions. The lower limit of integration is determined by the argument of the δ function; naturally, it will simply be $(\mu_V+\mu_M)^2$. In the present case the k^2 dependence of $W(x,y,k^2)$ is $(k^2)^n$, $n=0$, 1 and m takes on the values 0, 1, and 2. Since the σ^2 integration is cut off, the argument of the δ function in (3.19) cannot vanish for $k^2=\infty$. We thus find

$$\begin{aligned}\int_0^\infty k^2(k^2)^n\delta''\big([k^2+\beta(x)+\alpha(x)y]/y(x-y)-\sigma^2\big)dk^2 &= y^2(x-y)^2\delta\big(\{\beta(x)+\alpha(x)y\}/y(x-y)-\sigma^2\big) \quad \text{for } n=0\\ &= 2y^3(x-y)^3\theta\big(\sigma^2y(x-y)-\{\beta(x)+\alpha(x)y\}\big) \quad \text{for } n=1\,.\end{aligned} \tag{3.20}$$

At $q^2=0$ we then have the following results:

$$R(0) = \frac{1}{2}\int_0^1 dx\int_0^x dy\, W(x,y)\mathfrak{F}_{m,n}(x,y)\theta\big(\Lambda^2-[\beta(x)+\alpha(x)y]/y(x-y)\big)\,, \tag{3.21}$$

where

$$\begin{aligned}\mathfrak{F}_{m,n}(x,y) &= [\beta(x)+\alpha(x)y]^{-1}, \quad m=0, n=0\\ &= -[y(x-y)]^{-1}, \quad m=1, n=0\\ &= [\beta(x)+\alpha(x)y]/y^2(x-y)^2, \quad m=2, n=0\\ &= 2\ln\{\Lambda^2y(x-y)/[\beta(x)+\alpha(x)y]\}, \quad m=0, n=1\\ &= -2\{\Lambda^2-[\beta(x)+\alpha(x)y]/y(x-y)\}, \quad m=1, n=1.\end{aligned} \tag{3.22}$$

$g_2(0)$ is then obtained by inserting from Appendix B the appropriate functions for $W(x,y)$. We shall refer to the calculation of $g_2(0)$ based on Eqs. (3.21) and (3.22) as the dispersion relation evaluation of the triangle graphs.

Let us now investigate the behavior of Eq. (3.21) as $\Lambda\to\infty$. We first consider the F_1G_1 term in $k^2H_2^{(a,b)}$. Here we want to evaluate

$$\begin{aligned}&\lim_{\Lambda\to\infty}(\mp)(2\mu_V^2)^{-1}\int_0^1 dx(1-\tfrac{3}{2}x)\int_0^x dy\ln\{\Lambda^2y(x-y)/[\beta(x)+\alpha(x)y]\}\theta\big(\Lambda^2-[\beta(x)+\alpha(x)y]/y(x-y)\big)\\ &\qquad = (\pm)(2\mu_V^2)^{-1}\int_0^1 dx(1-\tfrac{3}{2}x)[x\ln|x\alpha(x)+\beta(x)|+\beta(x)\ln|1+x\alpha(x)/\beta(x)|/\alpha(x)]\pm 1/(12\mu_V^2)\,.\end{aligned} \tag{3.23}$$

Thus the result is again finite, and one might expect the answer (3.23) to be the same as that obtained by the Feynman evaluation. This is not the case, however. One can verify that the Feynman evaluation of the F_1G_1 term in $k^2H_2^{(a,b)}$ yields only the first term in Eq. (3.23). Thus the dispersion and Feynman evaluations yield results differing by $(\pm)1/(12\mu_V^2)$. The origin of this discrepancy is not difficult to understand. In computing the dispersion result, we have taken the discontinuity from the triangle graph and then evaluated an unsubtracted dispersion relation. But does the triangle graph itself satisfy an unsubtracted dispersion relation? The answer is no. Consider the behavior as $|q^2|\to\infty$ of the (Feynman evaluation of the) present F_1G_1 term in $k^2H_2^{(a,b)}$. One finds

$$\lim_{|q^2|\to\infty}(\mp)(2\mu_V^2)^{-1}\int_0^\infty k^4dk^2\int_0^1 dx(1-\tfrac{3}{2}x)\int_0^x dy[k^2+q^2y(x-y)+\alpha(x)y+\beta(x)]^{-3} = -(\pm)1/(12\mu_V^2)\,. \tag{3.24}$$

Thus this term approaches a constant as $|q^2|\to\infty$, and consequently it can only satisfy a once-subtracted dispersion relation,

$$F(q^2)=F(0)-\frac{q^2}{\pi}\int_{\sigma_{\rm th}^2}^{\infty}\frac{\mathrm{Im}F(-\sigma^2)d\sigma^2}{\sigma^2(\sigma^2+q^2-i\epsilon)}\,. \tag{3.25}$$

Letting $|q^2|\to\infty$ in Eq. (3.25), we find

$$F(0)-F(\infty)=\frac{1}{\pi}\int_{\sigma_{\rm th}^2}^{\infty}d\sigma^2\mathrm{Im}F(-\sigma^2)/\sigma^2\,. \tag{3.26}$$

Thus the dispersion evaluation based on Eq. (1.9) should yield $F(0)-F(\infty)$. The explicit results in Eqs. (3.23) and (3.24) confirm this analysis.

In the dispersion evaluation the terms in $H_1^{(a,b)}$, except for those proportional to q^2 and q^4, are finite and the same as in the Feynman evaluation. The q^2 terms in general diverge, but the F_1G_1 term

$$\pm q^2y(x-y)(1-x)/2\mu_V^2 \tag{3.27}$$

is again finite. This term also satisfies a once-subtracted dispersion relation. Thus the net result is that in the dispersion evaluation the F_1G_1 contribution is finite but unequal to the finite result obtained in the Feynman evaluation, the F_1G_2 contribution is finite and equal in the two evaluations, and the F_2 contributions diverge logarithmically in both evaluations.

There are thus two problems to be solved before we can obtain numerical results for the pseudotensor form factor. First, we must determine a cutoff so that the F_2 contributions can be calculated. This is done in Sec. III D through consideration of the unitarity condition for the annihilation process $B_1+\bar{B}_2\to V+M$. Second, there is the problem of the poorly-behaved parts of the triangle diagram. In a renormalizable theory, where $g_2(q^2)$ does satisfy an unsubtracted dispersion relation, these terms would be canceled by additional contributions. One could then argue that these terms should be neglected in the evaluation of the dispersion integral. As we shall see in Sec. III E, the contributions to $g_2(0)$ from these poorly-behaved terms are small, and so our results are insensitive to whether these terms are included in the dispersion integral or not.

D. The Unitarity Condition

When the dispersion variable σ^2 exceeds $(m_1+m_2)^2$, $B_1\bar{B}_2$ annihilation into a vector (V) and a pseudoscalar (M) meson becomes a physical process, and the annihilation amplitude is bounded by unitarity. Here we will be concerned with the Born approximation to the annihilation amplitude. We define the transition matrix $\tilde{T}_{fi}$ for this process by

$$S_{fi}=\delta_{fi}-(2\pi)^4i\delta^{(4)}(p_1+p_2-q_1-q_2)\times(m_1m_2/4E_1E_2\omega_{q_1}\omega_{q_2}\Omega^4)^{1/2}\tilde{T}_{fi}\,. \tag{3.28}$$

Using the Lagrangians given in Eqs. (3.1) and (3.2), it is straightforward to write down the contributions to $\tilde{T}_{fi}$ for the two Born diagrams (cf. Fig. 2). The scattering amplitude $f_{\lambda_c;\lambda_a\lambda_b}(\theta,\phi)$, defined by

$$f_{\lambda_c;\lambda_a\lambda_b}(\theta,\phi)=-[(m_1m_2)^{1/2}/4\pi W]\tilde{T}_{fi}\,, \tag{3.29}$$

is expanded in helicity states following Jacob and Wick,[34,35]

$$f_{\lambda_c;\lambda_a\lambda_b}(\theta,\phi)=(4p^*q^*)^{-1/2}\times\sum_J(2J+1)\mathfrak{D}^J_{\lambda_a-\lambda_b,\lambda_c}(-\phi,-\theta,\phi)^*\times\langle\lambda_c|T^J(W)|\lambda_a\lambda_b\rangle\,. \tag{3.30}$$

λ_a and λ_b are the helicities of the initial baryon and antibaryon, and λ_c is the helicity of the final vector meson. The form factor $g_2(q^2)$ receives contributions only from $J^P=1^+$ states. Thus we want to invert Eq. (3.30). This is done using the orthogonality of the $d^J_{m'm}(\theta)$:

$$\langle\lambda_c|T^J(W)|\lambda_a\lambda_b\rangle=(4p^*q^*)^{1/2}\tfrac{1}{2}\times\int_{-1}^{1}d(\cos\theta)f_{\lambda_c;\lambda_a\lambda_b}(\theta,\phi)\times\mathfrak{D}^J_{\lambda_a-\lambda_b,\lambda_c}(-\phi,-\theta,\phi)\,. \tag{3.31}$$

Denote the $|VM\rangle$ state by $|1\rangle$ and the $|B_1\bar{B}_2\rangle$ state by $|2\rangle$. Then from the unitarity of the S matrix

$$\sum_\lambda\langle1,\lambda_\beta|S^J|1,\lambda\rangle^*\langle1,\lambda|S^J|1,\lambda_\alpha\rangle+\sum_{\lambda_1\lambda_2}\langle1,\lambda_\beta|S^J|2,\lambda_1\lambda_2\rangle^*\langle2,\lambda_1\lambda_2|S^J|1,\lambda_\alpha\rangle+\sum_{n\neq1,2}\langle1,\lambda_\beta|S^J|n\rangle^*\langle n|S^J|1,\lambda_\alpha\rangle=\delta_{\lambda_\alpha\lambda_\beta}\,. \tag{3.32}$$

Since $S=1+iT$, the unitarity condition (3.32) becomes (for $\lambda_\alpha=\lambda_\beta=\lambda_c$)

$$\sum_{\lambda_1\lambda_2}|\langle1,\lambda_c|T^J|2,\lambda_1\lambda_2\rangle|^2=1-\sum_\lambda|\langle1,\lambda|S^J|1,\lambda_c\rangle|^2-\sum_{n\neq1,2}|\langle n|T^J|1,\lambda_c\rangle|^2\leq1. \tag{3.33}$$

Since $\lambda_c = \pm 1, 0$, Eq. (3.33) contains three conditions for each J. There are only two independent constraints, however, since those for $\lambda_c = +1$ and $\lambda_c = -1$ are related by parity.

We consider first the $\Lambda\bar{p}$ annihilation. The helicity matrix elements are evaluated for the case $J=1$ using Eqs. (3.29) and (3.31) for each of the four VM states: $K^*\pi$, $K^*\eta$, ρK, and ϕK. The matrix elements for $K^*\pi$ and $K\rho$ are larger than for the other two states. Here the left-hand side of Eq. (3.33) exceeds unity for $\lambda_c = \pm 1$ when σ is only a few tenths of 1 MeV above threshold and for $\lambda_c = 0$ when $\sigma \sim 100$ MeV above threshold. When $\sigma = 2.5$ GeV the left-hand side has reached ~60 for $\lambda_c = \pm 1$ and ~10 for $\lambda_c = 0$ (see Ref. 36). It is interesting to note that the violation of unitarity is milder if only the charge coupling $(G_1\gamma_\mu)$ of vector mesons to baryons is retained. In this case at $\sigma = 2.5$ GeV the left-hand side ~10 for $\lambda_c = \pm 1$, while the unitarity limit is never violated for $\lambda_c = 0$. The results for $\Sigma^-\bar{n}$ annihilation[37] are similar to those for $\Lambda\bar{p}$.

For $\Sigma^- \to \Lambda e^-\bar{\nu}_e$ only the states $\bar{K}^*K$, $\rho\pi$, and $K^*\bar{K}$ can couple to the axial current via a first-class coupling, and these are the states we include in the unitarity sum. The first two give the larger contribution. The violation of Eq. (3.33) is much less severe than it was for $\Lambda\bar{p}$. For both $\lambda_c = \pm 1$ and $\lambda_c = 0$, the left side exceeds unity at 300–400 MeV above threshold. It does not become as big as 10 until $\sigma \sim 4$ GeV.

It is thus apparent that the Born diagram does not provide a very good description of $B\bar{B} \to VM$ annihilation in the physical region. As a consequence the region $\sigma^2 > (m_B + m_{\bar{B}})^2$ will contribute far too much to $g_2(q^2)$ if the integral in Eq. (1.9) is not cut off. The present discussion suggests that the cutoff should be chosen near the annihilation threshold, $\Lambda \approx m_B + m_{\bar{B}}$. The explicit dependence of the results on the cutoff is discussed in Sec. III E.

E. Numerical Results—SU(3)-Invariant Couplings

We now discuss the values obtained for $g_2(0)$ from the meson triangle diagram using the SU(3)-invariant couplings discussed in Sec. III A. From the discussion in Secs. III C and III D there are two effects that are of particular interest. One is the contribution to the dispersion integral of the poorly-behaved terms in the triangle graph, and the other is the dependence on the dispersion cutoff.

Tables II and III give values of $g_2(0)/f_1(0)$ for the decays $\Lambda \to p l^-\bar{\nu}_l$ and $\Sigma^- \to n l^-\bar{\nu}_l$, respectively. $f_1(0)$ is assumed to have its Cabibbo value (see Table I).[38] The first three rows in each table give values obtained from the dispersion relation evaluation for different values of the cutoff, $\Lambda = m_1 + m_2$, $\Lambda = 2.5$ GeV, and $\Lambda = \infty$. Although the F_2 terms diverge as $\Lambda \to \infty$, it is apparent that for reasonable values of Λ they are small compared to the F_1 terms. Note also that the F_1G_2 term varies by only 15–20% between $\Lambda = m_1 + m_2$ and $\Lambda = \infty$. The next three entries in the tables are values obtained from the dispersion evaluation, but with the poorly-behaved parts of the triangle graph omitted. We refer to this as the unsubtracted dispersion evaluation inasmuch as only those parts of the triangle graph that satisfy an unsubtracted dispersion relation are retained. The F_1G_2 term is unaltered from the regular dispersion evaluation. The F_1G_1 terms are reduced a fair amount, and the F_2 terms are somewhat more important, but the total values for $g_2(0)$ are nearly the same as before. One can thus conclude that the poorly-behaved parts of the triangle diagram do not appreciably affect the determination of $g_2(0)$. The final entry in Tables II and III gives the results of the Feynman evaluation of the triangle graph.[39]

In the following we shall use as representative the values obtained from the dispersion evaluation

TABLE II. Ratio of induced pseudotensor to vector form factors, $g_2(0)/f_1(0)$, as a function of cutoff and method of evaluation for the decay $\Lambda \to p + l^- + \bar{\nu}_l$. For each entry the contributions proportional to the four couplings F_1G_1, F_1G_2, F_2G_1, and F_2G_2 are given as well as the total contribution.

Evaluation method	F_1G_1	F_1G_2	F_2G_1	F_2G_2	Total
Dispersion					
$\Lambda = m_\Lambda + m_p$	−0.116	0.114	0.007	0.017	0.022
$\Lambda = 2.5$	−0.100	0.128	0.014	0.024	0.066
$\Lambda = \infty$	−0.056	0.140	∞	∞	∞
Unsubtracted dispersion					
$\Lambda = m_\Lambda + m_p$	−0.079	0.114	−0.022	0.010	0.023
$\Lambda = 2.5$	−0.060	0.128	−0.026	0.015	0.057
$\Lambda = \infty$	−0.024	0.140	−0.025	0.051	0.142
Feynman	−0.122	0.140	∞	∞	∞

TABLE III. Same as Table II except for the decay $\Sigma^- \to n + l^- + \bar{\nu}_l$.

Evaluation method	F_1G_1	F_1G_2	F_2G_1	F_2G_2	Total
Dispersion					
$\Lambda = m_{\Sigma^-} + m_n$	0.090	0.082	−0.002	0.012	0.182
$\Lambda = 2.5$	0.086	0.086	−0.004	0.015	0.183
$\Lambda = \infty$	0.066	0.094	∞	∞	∞
Unsubtracted dispersion					
$\Lambda = m_{\Sigma^-} + m_n$	0.061	0.082	0.012	−0.003	0.152
$\Lambda = 2.5$	0.050	0.086	0.014	−0.004	0.146
$\Lambda = \infty$	−0.015	0.094	0.012	−0.013	0.078
Feynman	−0.022	0.094	∞	∞	∞

(including all terms) with a cutoff $\Lambda = 2.5$ GeV. The values of $g_2(0)$ for the two decays are then

$$[g_2(0)/f_1(0)]_{\Lambda p} = 0.066,$$
$$[g_2(0)/f_1(0)]_{\Sigma^- n} = 0.183. \tag{3.34}$$

The small value for $g_2(0)$ in Λ beta decay actually arises from large cancellations among the various intermediate states. The contributions from these individual diagrams are shown in Tables IV and V for the $\Lambda \to p$ and $\Sigma^- \to n$ decays. As we have mentioned previously, contributions from individual states need not vanish in the SU(3) limit, and thus they can be relatively large. It is only the sum over all states that must vanish in the SU(3) limit. It should also be noted that although the F_1G_2 contribution summed over all states is relatively independent of Λ (cf. Tables II and III), the individual contributions show a much greater variation with Λ. Thus for $\Lambda = 2.5$ GeV the $K^*\pi$ and ρK states have reached only ~50% of their asymptotic ($\Lambda = \infty$) values, and the $K^*\eta$ and ϕK states only ~30–35 %.

Table VI gives the individual contributions to $g_2(0)$ for the decay $\Sigma^- \to \Lambda l^- \bar{\nu}_l$. The values are again obtained from the dispersion evaluation with a cutoff $\Lambda = 2.5$ GeV. Here the $\rho\pi$ states are much more important than the K^*K states. The final value for $g_2(0)$, which also holds for the $\Sigma^+ \to \Lambda$ decay, is considerably larger than in the previous two cases:

$$[g_2(0)/g_1(0)]_{\Sigma^\pm \Lambda} = -0.590. \tag{3.35}$$

There are two additional independent $\Delta S = 1$ beta decays in the baryon octet, namely $\Xi^- \to \Lambda$ and $\Xi^0 \to \Sigma^+$. [The decays $\Sigma^0 \to p$ and $\Xi^- \to \Sigma^0$ are then determined by the $\Delta T = \frac{1}{2}$ nature of the current: $(\Sigma^0 \to p) = (\frac{1}{2})^{1/2}(\Sigma^- \to n)$ and $(\Xi^- \to \Sigma^0) = (\frac{1}{2})^{1/2}(\Xi^0 \to \Sigma^+)$.] Using the same procedures as before, we find the following values of $g_2(0)$ for these decays:

$$[g_2(0)/f_1(0)]_{\Xi^- \Lambda} = 0.024,$$
$$[g_2(0)/f_1(0)]_{\Xi^0 \Sigma^+} = 0.336. \tag{3.36}$$

Under the assumptions (i) that the weak vector currents and the electromagnetic current belong to the same unitary octet, and (ii) that the breaking of unitary symmetry is due to a term behaving like the eighth component of an octet, Ademollo and Gatto[40,14] derived two sum rules for the induced second-class contributions [i.e., $f_3(q^2)$ or $g_2(q^2)$] to these decays. They are

$$\sqrt{6}[(\Lambda \to p) + (\Sigma^- \to \Lambda)] = (\Sigma^- \to n) + 2(\Xi^0 \to \Sigma^+), \tag{3.37}$$

TABLE IV. Ratio of induced pseudotensor to vector form factors, $g_2(0)/f_1(0)$, for the decay $\Lambda \to p + l^- + \bar{\nu}_l$. The values are obtained from the dispersion evaluation using a cutoff of 2.5 GeV. For each triangle graph, the contributions proportional to the four couplings F_1G_1, F_1G_2, F_2G_1, and F_2G_2 are given as well as the total contribution.

Triangle graph	F_1G_1	F_1G_2	F_2G_1	F_2G_2	Total
$K^*\pi N$	−0.417	0.182	0.013	0.075	−0.147
$\pi K^*\Sigma$	−0.137	−0.079	−0.006	−0.018	−0.240
$\rho K\Sigma$	0	0.035	0	0.010	0.045
$K\rho N$	0.245	−0.053	0.001	−0.059	0.134
$K^*\eta N$	−0.046	0.012	0.000	0.007	−0.027
$\eta K^*\Lambda$	0.098	−0.026	0.005	−0.009	0.068
$\phi K\Lambda$	0	0.056	0	0.017	0.073
$K\phi N$	0.157	0.001	0.001	0.001	0.160
Sum of all graphs	−0.100	0.128	0.014	0.024	0.066

TABLE V. Same as Table IV except for the decay $\Sigma^- \to n + l^- + \bar{\nu}_l$.

Triangle graph	F_1G_1	F_1G_2	F_2G_1	F_2G_2	Total
$K^*\pi N$	0.147	0.071	−0.007	0.033	0.244
$\pi K^*\Sigma$	0.181	0.083	0.006	0.021	0.291
$\pi K^*\Lambda$	−0.168	0.052	−0.003	0.018	−0.101
$\rho K\Sigma$	0.107	−0.021	0.004	−0.006	0.084
$\rho K\Lambda$	0	−0.081	0	−0.030	−0.111
$K\rho N$	0.038	−0.002	−0.000	−0.009	0.027
$K^*\eta N$	−0.048	−0.014	0.001	−0.009	−0.070
$\eta K^*\Sigma$	−0.097	−0.028	−0.006	−0.009	−0.140
$\phi K\Sigma$	0	0.026	0	0.007	0.033
$K\phi N$	−0.074	−0.000	0.001	−0.001	−0.074
Sum of all graphs	0.086	0.086	−0.004	0.015	0.183

TABLE VI. Ratio of induced pseudotensor to axial-vector form factors, $g_2(0)/g_1(0)$, for the decay $\Sigma^- \to \Lambda + l^- + \bar{\nu}_l$. The values are obtained from the dispersion evaluation using a cutoff of 2.5 GeV.

Triangle graph	F_1G_1	F_1G_2	F_2G_1	F_2G_2	Total
$\rho\pi\Sigma$	−1.137	0.226	−0.011	0.074	−0.848
$\pi\rho\Sigma$	0	−0.396	0	−0.139	−0.535
$\bar{K}^*\bar{K}N$	0.279	0.033	−0.012	0.052	0.352
$\bar{K}\bar{K}^*N$	0.124	−0.003	−0.005	−0.019	0.097
$K^*K\Xi$	−0.052	0.043	−0.003	0.012	−0.000
$KK^*\Xi$	0.315	0.007	0.019	0.003	0.344
Sum of all graphs	−0.471	−0.090	−0.012	−0.017	−0.590

and

$$\sqrt{6}\,[(\Lambda \to p) - (\Xi^- \to \Lambda)] = -(\Sigma^- \to n) + (\Xi^0 \to \Sigma^+)\,. \tag{3.38}$$

In the present calculation g_2 is determined by the product of mass breakings in three different octets, and so the sum rules (3.37) and (3.38) need not remain valid. Using the results for $g_2(0)$ in Eqs. (3.34)–(3.36), we can see to what extent they are violated.[41] The left-hand side of (3.37) is $\sqrt{6}\,(-0.081 - 0.373) = -1.112$, while the right-hand side is $-0.183 - 0.672 = -0.855$. For (3.38) the left-hand side is $\sqrt{6}\,(-0.081 + 0.029) = -0.127$, and the right-hand side is $0.183 - 0.336 = -0.153$. Thus for (3.37) the fractional deviation is about 26%, and for (3.38) it is only 7%. So the sum rules are not too badly violated.

F. Breaking of SU(3) Couplings

So far only the mass breaking of SU(3) has been considered. But coupling constants can also deviate from their SU(3) values, and this provides an additional contribution to the induced pseudotensor term. In contrast to the mass breakings, coupling constant breakings are generally known very poorly. It is conventional to assume that the couplings are broken only to second order in SU(3) while the masses are broken in first order. If this is the case, then the coupling-constant contribution to $g_2(q^2)$ should be unimportant compared to the mass contribution. For some of the coupling constants, however, the deviations appear to be considerably larger than second order. Thus a recent estimate of the $\Sigma\Lambda\pi$ coupling gives $g_{\Sigma\Lambda\pi}{}^2/4\pi = 11.4 \pm 1.2$,[42] whereas the SU(3) prediction is $g_{\Sigma\Lambda\pi}{}^2/4\pi = \frac{4}{3}\,\alpha_M{}^2(g_{\pi NN}{}^2/4\pi) = 7.6$. This is a discrepancy of 23% in $g_{\Sigma\Lambda\pi}$. It thus appears to be necessary to investigate the coupling constant contribution in more detail. Since we have only a limited knowledge of the breaking of SU(3) couplings, we will not be able to obtain a definite value of $g_2(0)$ as we did for the mass contribution. Instead, we shall merely make some rough estimates of the coupling contribution.

For some of the couplings it is possible to estimate the deviation, if any, from the SU(3) value. Certain couplings were used in determining the SU(3) parameters in Sec. III A, and so they are considered unbroken. These include the πNN, ρNN, axial-vector–$K^*\pi$, and axial-vector–$\rho\pi$ couplings. From the e^+e^- colliding-beam results of $\gamma_\phi{}^2/4\pi = 2.8 \pm 0.2$ and $\gamma_\omega{}^2/4\pi = 4.8 \pm 0.5$,[43] one finds $\gamma_{\phi_8}{}^2/4\pi = 1.77 \pm 0.11$. This is consistent with the SU(3) prediction $\gamma_{\phi_8}{}^2/4\pi = 3[\gamma_\rho{}^2/4\pi] = 1.92 \pm 0.15$.[24] With our assumption of vector-meson dominance, the couplings of the ρ and ϕ mesons are related to the electromagnetic form factors of the baryons:

$$G_{1,2}^{\bar{B}B(\rho,\phi)} = 4\hat{\gamma}_{(\rho,\phi)} F_{1,2}^{\bar{B}B(\rho,\phi)}(0)\,. \tag{3.39}$$

The values of $F_1(0)$ are determined by the electric charge and so are unaltered by SU(3) breaking. Thus the $\Lambda\Lambda\phi$, $\Sigma\Sigma\phi$, and $\Sigma\Lambda\rho$ charge couplings remain zero. For the magnetic moments the proton and neutron values are accurately known and determine the SU(3) parameters. The Λ moment (in particle magnetons) is then predicted to be -0.96. The experimental value is -0.80 ± 0.07.[44] This determines the broken value of $G_2^{\Lambda\Lambda\phi}$. Since only the Σ^+ moment is known experimentally,[44] one can determine only the sum $G_2^{\Sigma\Sigma\rho} + (\frac{1}{3})^{1/2} G_2^{\Sigma\Sigma\phi}$. From Kp dispersion relations one estimates the quantity $\bar{g}^2 \equiv g_{p\Lambda K}{}^2 + 0.92\, g_{p\Sigma K}{}^2$ to be $\bar{g}^2/4\pi = 14.2 \pm 1.2$.[45] We then assume $g_{p\Lambda K}{}^2/4\pi \cong 13$ and $g_{p\Sigma K}{}^2/4\pi \lesssim 3$. The SU(3) predictions are 14.9 and 0.91, respectively. Other values employed are $g_{\Sigma\Lambda\pi}{}^2/4\pi = 11.4 \pm 1.2$ (see Ref. 42), $g_{\Sigma\Sigma\pi}{}^2/4\pi = 12.5 \pm 2.0$ (see Ref. 46), and $g_{\eta NN}{}^2/4\pi = 2.6 \pm 0.9$ (see Ref. 47), to be compared with the SU(3) predictions of 7.6, 8.2 and 1.2. For the remaining couplings we allow a variation of 20% from the SU(3) value. We then follow two different procedures to compute the effect on $g_2(0)$. First, we estimate the one-standard-deviation uncertainty arising from these 20% variations. Together with the SU(3)-broken couplings discussed above, this leads to the following results for $g_2(0)$:

$$\begin{aligned} &[g_2(0)/f_1(0)]_{\Lambda p} = -0.04 \pm 0.12, \\ &[g_2(0)/f_1(0)]_{\Sigma^- n} = 0.20 \pm 0.10, \\ &[g_2(0)/g_1(0)]_{\Sigma^\pm\Lambda} = -0.93 \pm 0.23\,. \end{aligned} \tag{3.40}$$

The differences between these values for $g_2(0)$ and those arising from the mass breaking alone [see Eqs. (3.34) and (3.35)] are comparable to the errors in (3.40) arising from the uncertainty in the coupling breakings. It will be useful for the comparison with experiment to have an estimate of the largest value of $g_2(0)$ that can result from the meson triangle graph. Thus in a second computation we systematically choose the 20% variation in each unknown coupling so as to maximize $|g_2(0)|$. This procedure leads to the following limits:

$$\begin{aligned} &-0.4 < [g_2(0)/f_1(0)]_{\Lambda p} < 0.2, \\ &-0.1 < [g_2(0)/f_1(0)]_{\Sigma^- n} < 0.5, \\ &-1.5 < [g_2(0)/g_1(0)]_{\Sigma^\pm\Lambda} < -0.3\,. \end{aligned} \tag{3.41}$$

These limits on $g_2(0)$ arising from the coupling breaking represent something like a 98% confidence level. Thus the observation of values of $g_2(0)$ outside these ranges would constitute strong evidence for either some mechanism other than the meson triangle graph inducing the pseudotensor term or, more probably, the presence of a second-class interaction in the weak Hamiltonian.

G. Effects of Axial-Vector Resonances

As we saw earlier, the existence of the ρ meson was crucial to the explanation of the anomalous isovector magnetic moment of the nucleon in terms of the two-pion state. Since axial-vector mesons are also known to exist, it is of interest to consider their effect on the pseudotensor form factor. To obtain a rough estimate of the resonance effect, we shall employ the analog of Eq. (2.3), that is

$$\mathrm{Im}g_2(-\sigma^2) \approx |F_{1,2}(-\sigma^2)/F_{1,2}(0)|^2 [\mathrm{Im}g_2(-\sigma^2)]_0 , \tag{3.42}$$

where $F_{1,2}(q^2)$ are the axial form factors defined in Eq. (3.8) and $[\mathrm{Im}g_2(-\sigma^2)]_0$ is the discontinuity as calculated previously from the triangle graph. Explicit expressions for the form factors can be obtained from the current algebra analysis in Appendix A of the axial-vector–pseudoscalar vertex. For the case of the strangeness-changing current, which contains the K_A pole, we derive from Eq. (A9) with the approximations (A12) and (A13) the following expressions:

$$F_1(-\sigma^2) = \sqrt{2}\, m_{K^*}[1 + (m_{K_A}/2m_{A_1})\{\sigma^2 - m_{K^*}^2 + \tfrac{1}{2}\delta_{K^*}(\sigma^2 - m_{K^*}^2 - m_\pi^2)\}/(m_{K_A}^2 - \sigma^2)], \tag{3.43}$$

$$F_2(-\sigma^2) = F_2(0) m_{K_A}^2/(m_{K_A}^2 - \sigma^2) . \tag{3.44}$$

The K_A meson has a mass of 1243 ± 8 MeV and a width $\Gamma = 70^{+26}_{-18}$ MeV.[48] Thus, of the meson channels we are considering, only the $K^*\pi$ is completely open at the K_A mass. (The mass of the ρK system is ≈ 1260 MeV; the large width of the ρ will bring the effective threshold somewhat below the K_A mass.) Consequently, the resonance effects will be most pronounced in this channel. To include the finite width of the K_A, we make the replacement

$$m_{K_A}^2 - \sigma^2 \to m_{K_A}^2 - \sigma^2 - i m_{K_A} \Gamma (p/p_{K_A})(m_{K_A}/\sigma) \tag{3.45}$$

in the denominator of Eqs. (3.43) and (3.44). Here p is the decay three-momentum in the K_A rest frame.

There is an important difference between the expressions for $F_1(-\sigma^2)$ and for $F_2(-\sigma^2)$. Equation (3.43) for F_1 contains a subtraction constant in addition to the K_A pole, while Eq. (3.44) for F_2 contains only the pole. This leads to a marked contrast in the resonant behavior of the two form factors. Thus while $|F_2(-\sigma^2)/F_2(0)|^2$ peaks at a value of around 320 at the resonance, the peak value for $|F_1(-\sigma^2)/F_1(0)|^2$ is only about 17. The behavior of the triangle graph discontinuity as a function of σ is much smoother. The F_1 terms rise from threshold, reach their maximum in the range 1200–1300 MeV, and then fall off slowly. The F_2 terms continue to increase beyond the threshold region. Using the approximation (3.42), one finds that the contribution of the $K^*\pi$ states to the F_1 term in $g_2(0)/f_1(0)$ for the $\Lambda \to p$ decay is increased considerably, from -0.451 to -0.944. Similarly, the contribution of the same states to F_2 is increased from 0.064 to 0.480. While these estimates of the resonance effect may not be too reliable, particularly for the F_2 terms, it is interesting to note that the total $K^*\pi$ contribution is only slightly altered, from -0.387 to -0.464. Thus one will still have a small value of $g_2(0)$ for the $\Lambda \to p$ decay. For the $\Sigma^- \to n$ decay, the $K^*\pi$ contributions to F_1 and F_2 have the same sign, and their sum is increased from 0.434 to 0.987. Thus the value of $g_2(0)$ could be raised considerably. Judging from the anomalous moment calculation, however, one expects the approximation (3.42) to overestimate the resonance effect. It thus seems reasonable to conclude that at worst the resonance effects are no larger than the upper limits arising from the uncertainty in the coupling breaking given in Eq. (3.41). A more refined calculation should include a better treatment of both of these topics.

IV. HIGHER-MASS STATES

In the dispersion calculation of the isovector magnetic moment, the two-pion cut (beginning at $q^2 = -4\mu^2$) is four times as close to $q^2 = 0$ as the

next higher singularity (the four-pion cut beginning at $q^2=-16\mu^2$). For the pseudotensor form factor, however, the separation of the lowest-mass quasi-two-body states from higher-mass states relative to $q^2=0$ is not so pronounced. For example, the $K_A\pi$ state occurs at $\approx$1380 MeV, which is only $\approx$350 MeV greater than the $K^*\pi$ state and actually $\approx$60 MeV less than the $K^*\eta$ and $\phi_8 K$ states. Thus it is not clear how reliable the approximation of keeping only the lowest-mass states should be. To investigate this question, we consider in this section the tensor-pseudoscalar meson and baryon-antibaryon states. We choose the tensor mesons rather than the somewhat less massive axial-vector mesons since the coupling constants are better known for the former.

A. Tensor Mesons

We again evaluate the triangle diagrams in Fig. 2, only now with tensor instead of vector mesons. The pseudoscalar-baryon coupling is given in Eq. (3.1). For the coupling of the f meson to the nucleons, we assume a vertex of the form

$$\langle N(p_2)|f|N(p_1)\rangle=\bar{u}(p_2)[iG_1^{fN\bar{N}}(P_\mu\gamma_\nu+P_\nu\gamma_\mu)/4m+G_2^{fN\bar{N}}P_\mu P_\nu/4m^2]u(p_1)\epsilon_{\mu\nu}\,, \tag{4.1}$$

where $P_\mu\equiv(p_1+p_2)_\mu$ and $\epsilon_{\mu\nu}$ is the (symmetric) meson polarization tensor. A similar vertex is assumed for the f' coupling to the nucleons. Using f and f' dominance of the energy-momentum tensor and assuming that the f' decouples from nucleons (as suggested by the quark model), Renner[49] has obtained the results

$$|G_1^{fN\bar{N}}|\cong 8.7\pm0.5,\quad G_2^{fN\bar{N}}\cong 0\,. \tag{4.2}$$

Use of πN backward dispersion relations yields a value for $G_1^{fN\bar{N}}$ approximately three times as large,[50] so (4.2) should probably be considered only a rough estimate. We next need to obtain the coupling of the tensor octet to the baryons. Exchange degeneracy suggests that the F/D ratios for these couplings should be the same as for the vector couplings to the baryons.[51] This leads to the decoupling of the f' (and the ϕ) from nucleons. Thus we have

$$\langle B^k(p_2)|T^i|B^j(p_1)\rangle=\bar{u}_k(p_2)[iG_1^T if_{ijk}(P_\mu\gamma_\nu+P_\nu\gamma_\mu)/2(m_j+m_k)+G_2^T\{(1-\alpha_V)if_{ijk}+\alpha_V d_{ijk}\}P_\mu P_\nu/(m_j+m_k)^2]$$
$$\times u_j(p_1)\epsilon_{\mu\nu}\,. \tag{4.3}$$

We assume f-f' mixing,

$$f'=f_8\cos\theta-f_1\sin\theta,\quad f=f_8\sin\theta+f_1\cos\theta\,. \tag{4.4}$$

The Gell-Mann–Okubo mass formula (in mass squared) yields $\mu_8=1456$ MeV, $\mu_1=1335$ MeV, and $\theta=30.1°$. For the mixing angle θ, however, we prefer to use the quark model prediction, $\theta=\sin^{-1}(\frac{1}{3})^{1/2}=35.3°$. From Eqs. (4.2)–(4.4) and the decoupling of the f', we then obtain

$$|G_1^T|=(\tfrac{4}{3})^{1/2}\sin\theta|G_1^{fN\bar{N}}|\cong 5.8,\quad G_2^T\cong 0\,. \tag{4.5}$$

For the coupling of the singlet tensor meson to the baryons we have

$$|G_1^{(1)}|=\cos\theta|G_1^{fN\bar{N}}|\cong 7.1,\quad G_2^{(1)}\cong 0\,. \tag{4.6}$$

Finally, we need to determine the matrix element of the axial current between tensor and pseudoscalar meson states. The general form of this matrix element is

$$(4\omega_M\omega_T\Omega^2)^{1/2}\langle M^k(k)|\sin\theta_C A_\mu^{(\Delta S=1)i}(0)|T^j(p)\rangle=\sin\theta_C id_{ijk}[F_1^T(q^2)\epsilon_{\mu\alpha}q_\alpha+F_2^T(q^2)p_\mu\epsilon_{\alpha\beta}q_\alpha q_\beta+F_3^T(q^2)q_\mu\epsilon_{\alpha\beta}q_\alpha q_\beta]\,, \tag{4.7}$$

where $q=p-k$. If we define $d_{0ij}=(\frac{2}{3})^{1/2}\delta_{ij}$, then (4.7) describes the coupling of the singlet mesons (f_1 and η') as well as the octets. Once again, the $F_3^T q_\mu$ term does not contribute to the induced pseudotensor form factor. Taking the divergence of the current in (4.7) and using kaon PCAC,

$$\partial_\mu A_\mu^i(x) = \mu_K^2 F_K \phi_K^i(x), \tag{4.8}$$

we have

$$(4\omega_M\omega_T\Omega^2)^{1/2}\langle M^k(k)|\phi_K^i(0)|T^j(p)\rangle = -(d_{ijk}/\mu_K^2 F_K)[F_1^T(q^2) + F_2^T(q^2)p\cdot q + F_3^T(q^2)q^2]\epsilon_{\alpha\beta}q_\alpha q_\beta . \tag{4.9}$$

Multiplying (4.9) by $(q^2+\mu_K^2)$ and taking the limit $q^2 \to -\mu_K^2$, we obtain the coupling for the decay of the tensor to two pseudoscalar mesons. This coupling has the general form

$$g_{TMM} q_\mu q_\nu \epsilon_{\mu\nu} d_{ijk}, \tag{4.10}$$

and the decay width is given by

$$\Gamma_{TMM} = g_{TMM}^2 k^5 (d_{ijk})^2/60\pi\mu_T^2 . \tag{4.11}$$

From (4.9) and (4.10) we find

$$g_{TMM} = \lim_{q^2\to-\mu_K^2} [-(q^2+\mu_K^2)/\mu_K^2 F_K] \times [F_1^T(q^2) + F_2^T(q^2)p\cdot q + F_3^T(q^2)q^2]. \tag{4.12}$$

Assuming that Eq. (4.12) can be continued to $q^2 = 0$, we have finally

$$F_K g_{TMM} = -[F_1^T(0) - \tfrac{1}{2}(\mu_T^2 - \mu_M^2)F_2^T(0)]. \tag{4.13}$$

In the decay of a tensor meson into an axial and a pseudoscalar meson, F_1^T corresponds to the P-wave and F_2^T to the F-wave decay. Judging by our results for the vector mesons, we expect the pseudotensor term to be dominated by the lower angular momentum state. Consequently, we shall neglect the F_2^T term in (4.7) when evaluating the triangle graph. From Eq. (4.13) we shall then approximate

$$F_1^T(0) \cong -F_K g_{TMM} . \tag{4.14}$$

From the decays $A_2 \to K\bar{K}$ and $K_N \to K\pi$, which do not involve singlet-octet mixing, we find $|g_{TMM}| \cong 16.5\ \mathrm{GeV}^{-1}$. We thus have the estimate

$$|F_1^T(0)| \cong 1.5 . \tag{4.15}$$

We shall also use this estimate, together with Eq. (4.7), for the matrix element of the $\Delta S = 0$ axial current in the $\Sigma^\pm \to \Lambda$ decays.

The evaluation of the triangle graph is carried out in the same manner as for the vector mesons. From the Feynman amplitude for the diagram the pseudotensor term is extracted, the discontinuity along the cut is determined, and the dispersion integral is evaluated up to some cutoff. The tensor meson polarization sum is given by

$$\sum_{\text{pol}} \epsilon_{\mu\nu}(q)\epsilon_{\rho\sigma}(q) = \tfrac{1}{2}Q_{\mu\rho}Q_{\nu\sigma} + \tfrac{1}{2}Q_{\mu\sigma}Q_{\nu\rho} - \tfrac{1}{3}Q_{\mu\nu}Q_{\rho\sigma}, \tag{4.16}$$

where

$$Q_{\mu\nu} = \delta_{\mu\nu} + q_\mu q_\nu/\mu_T^2 . \tag{4.17}$$

The dispersion evaluation of $g_2(q^2)$ diverges like Λ^4. We shall again choose $\Lambda = 2.5$ GeV. For this value the finite terms are comparable to or larger than the divergent ones. For values of $\Lambda > 2.5$ GeV the Λ^4 terms quickly dominate the answer. Table VII gives the contributions to $g_2(0)/f_1(0)$ from the individual diagrams for the $\Lambda \to p$ and $\Sigma^- \to n$ decays. Note that the contributions from the octet and singlet states are of opposite sign and thus tend to cancel. (The *over-all* sign of the tensor contribution is not determined in the present analysis.) This makes the final values of $g_2(0)$ obtained from the tensor states quite small:

$$\begin{aligned} &|g_2(0)/f_1(0)|_{\Lambda p}^T = 0.025 , \\ &|g_2(0)/f_1(0)|_{\Sigma n}^T = 0.015 , \\ &|g_2(0)/g_1(0)|_{\Sigma\pm\Lambda}^T = 0.025 . \end{aligned} \tag{4.18}$$

TABLE VII. Tensor-meson contribution to the ratio $g_2(0)/f_1(0)$ for the decays $\Lambda \to p + l^- + \bar{\nu}_l$ and $\Sigma^- \to n + l^- + \bar{\nu}_l$. The values are obtained using a cutoff of 2.5 GeV. Contributions involving octet and singlet tensor mesons are shown separately.

$\Lambda \to p$		$\Sigma^- \to n$	
Graph	$g_2(0)/f_1(0)$	Graph	$g_2(0)/f_1(0)$
$K_N\pi N$	−0.213	$K_N\pi N$	0.074
$\pi K_N\Sigma$	0.071	$\pi K_N\Sigma$	−0.093
$A_2K\Sigma$	0	$\pi K_N\Lambda$	0.088
KA_2N	0.127	$A_2K\Sigma$	−0.049
$K_N\eta N$	0.005	$A_2K\Lambda$	0
$\eta K_N\Lambda$	0.011	KA_2N	0.020
$f_8K\Lambda$	0	$K_N\eta N$	0.005
Kf_8N	−0.020	$\eta K_N\Sigma$	−0.011
		$f_8K\Sigma$	0
Sum of octet states	−0.019	Kf_8N	0.009
		Sum of octet states	0.043
$f_1K\Lambda$	−0.106	$f_1K\Sigma$	0.043
Kf_1N	0.150	Kf_1N	−0.071
Sum of singlet states	0.044	Sum of singlet states	−0.028
Sum of singlet and octet	0.025	Sum of singlet and octet	0.015

Comparing with the results in Eqs. (3.34) and (3.35), we see that the tensor contribution is negligible for the $\Sigma^- \to n$ and $\Sigma^\pm \to \Lambda$ decays. This would still be true even if we used an $fN\bar{N}$ coupling as large as that suggested by the analysis of πN backward dispersion relations.[50] For $\Lambda \to p$ the tensor contribution is somewhat smaller than the (already small) vector contribution.

Once again, breaking of SU(3) coupling constants can lead to larger values of g_2 than those arising from mass breaking alone. Proceeding in the same manner as in Sec. III F, we find the following limits on the tensor contribution to $g_2(0)$:

$$\begin{aligned} &|g_2(0)/f_1(0)|^T_{\Lambda p} < 0.2 \\ &|g_2(0)/f_1(0)|^T_{\Sigma^- n} < 0.1 \\ &|g_2(0)/g_1(0)|^T_{\Sigma^\pm \Lambda} < 0.3 . \end{aligned} \tag{4.19}$$

These limits are generally small compared to those for the vector contributions given in Eq. (3.41).

B. Baryon-Antibaryon Pairs

As a second example of a higher-mass state, we consider the role of baryon-antibaryon pairs. These states are considerably more massive than the meson states considered previously, but they are included since it is relatively easy to obtain a first estimate of their contribution to $g_2(q^2)$. Here, there is only a single triangle diagram to consider, namely, the analog of that in Fig. 1(b). The axial current couples to the $B\bar{B}$ pair, and the pair then scatters via pseudoscalar-meson exchange. The pseudoscalar-baryon coupling is again taken from Eq. (3.1). The axial-$B\bar{B}$ vertex in the triangle graph is precisely the coupling that one is trying to compute, and thus one is generating an integral equation. As a first approximation we assume a $g_1(0)\gamma_\mu\gamma_5$ coupling at this vertex, where $g_1(0)$ takes its Cabibbo value. The $g_3(0)q_\mu\gamma_5$ coupling does not contribute to the induced pseudotensor term. The evaluation of the triangle graph is straightforward. The contribution to $g_2(0)$ is finite, and the Feynman and dispersion relation evaluations are equivalent. The resulting values for $g_2(0)$ are

$$\begin{aligned} &[g_2(0)/f_1(0)]^{B\bar{B}}_{\Lambda p} = 0.026 , \\ &[g_2(0)/f_1(0)]^{B\bar{B}}_{\Sigma^- n} = -0.004 , \\ &[g_2(0)/g_1(0)]^{B\bar{B}}_{\Sigma^\pm \Lambda} = 0.005 . \end{aligned} \tag{4.20}$$

These values are obtained without introducing a cutoff in the dispersion integral, and thus they probably overestimate the $B\bar{B}$ contribution to $g_2(0)$. Even so, the results in Eq. (4.20) are quite small compared to those obtained from the vector-pseudoscalar states [Eqs. (3.34) and (3.35)]. Furthermore, SU(3)-coupling breaking is unimportant for the $B\bar{B}$ states. The reason for this is that here the contribution to g_2 from *each* SU(3) state vanishes in the symmetry limit. Consequently, the small values in Eq. (4.20) result from a sum over small terms rather than from a cancellation among large terms. The results are thus fairly insensitive to deviations of the coupling constants from the SU(3) values. The conclusion seems to be that the $B\bar{B}$ state plays a negligible role in the determination of the induced pseudotensor form factor.

V. SUMMARY AND COMPARISON WITH EXPERIMENT

Before turning to the experimental situation, let us summarize the results we have obtained. We have attempted to estimate the induced pseudotensor term to be expected on the basis of SU(3)-symmetry breaking for several hyperon beta decays. These estimates were based on a simple dispersion-theory calculation. The pseudotensor form factor $g_2(q^2)$ was assumed to obey an unsubtracted dispersion relation, and the dispersion integral was assumed to be dominated by the lowest-mass states. The discontinuity under the integral arising from the vector-pseudoscalar meson states was obtained from the triangle graph in which single-baryon exchange was retained as the scattering mechanism. Since single-baryon exchange violates unitarity in $B\bar{B}$ annihilation, a cutoff was introduced in the dispersion integral. Using SU(3)-invariant couplings but physical values for all masses, we found the results for $g_2(0)$ given in Eqs. (3.34) and (3.35). We then attempted to estimate the effect of the breaking of SU(3) couplings. This led to the following values for $g_2(0)$:

$$\begin{aligned} &[g_2(0)/f_1(0)]_{\Lambda p} = -0.04 \pm 0.12 , \\ &[g_2(0)/f_1(0)]_{\Sigma^- n} = 0.20 \pm 0.10 , \\ &[g_2(0)/g_1(0)]_{\Sigma^\pm \Lambda} = -0.93 \pm 0.23 . \end{aligned} \tag{5.1}$$

The errors reflect the uncertainty in our knowledge of the coupling breakings. A similar treatment of the tensor-pseudoscalar meson and baryon-antibaryon states led to much smaller values of $|g_2(0)|$, particularly for the $\Sigma^- \to n$ and $\Sigma^\pm \to \Lambda$ decays. This provides support for our assumption that the vector-pseudoscalar states furnish the

major contribution to $g_2(0)$. We thus consider the results (5.1) to be probable values for $g_2(0)$ arising from SU(3)-symmetry breaking. It is possible that SU(3) breaking could generate much larger values of $g_2(0)$. This could result from a conspiracy in the way in which the various SU(3) couplings are broken or from a large enhancement of one of the intermediate states due to a resonance effect. These possibilities were discussed in Secs. III F and III G. Thus to have convincing evidence for the presence of a second-class interaction in the weak Hamiltonian, one would have to observe values of $g_2(0)$ more than two or three standard deviations away from the values in (5.1).

Of the hyperon leptonic decays we have considered, the most extensively investigated experimentally is $\Lambda \to p + e^- + \bar{\nu}_e$. Here two experiments involving the decay of polarized Λ's have been performed recently, one by an Argonne-Chicago-Ohio State-Washington collaboration[3,4] and one by a CERN-Heidelberg group.[5,6] In these experiments the electron, neutrino, and proton asymmetries with respect to the Λ polarization were measured as well as the decay rate and electron-neutrino correlation. The knowledge of these asymmetries permits a more complete investigation of the hadronic matrix element, Eq. (1.4). In 1971 Garcia[7] performed an extensive analysis of the data then existing. This included approximately one-third of the Argonne events[3] and all the CERN data[5] except for the neutrino asymmetry, which was obtained only later after reconstruction of the individual events.[6] Garcia first made a fit with f_1, f_2, and g_1 as parameters but g_2 set equal to zero. The q^2 dependence of the form factors was neglected. He found a solution very close to the Cabibbo-model predictions (cf. Table I):

$$\begin{aligned} &|f_1| = 0.30 \pm 0.02, \\ &f_2/f_1 = 1.5 \pm 1.5, \\ &g_1/f_1 = 0.70 \pm 0.06. \end{aligned} \tag{5.2}$$

The χ^2 for this fit was 4.94. With 2 degrees of freedom, this corresponds to a probability of only 9%. When g_2 was also allowed to vary, Garcia found a much better fit. χ^2 was reduced to 0.56, representing a probability of 47%. The values obtained were

$$\begin{aligned} &|f_1| = 0.36 \pm 0.01, \\ &f_2/f_1 = -2.6 \pm 2.0, \\ &g_1/f_1 = 0.19 \pm 0.14, \\ &g_2/f_1 = -4.6 \pm 1.5. \end{aligned} \tag{5.3}$$

Thus this improved fit involves a very large pseudotensor form factor. Comparing with Eq. (5.1), we see that this value is much more than an order of magnitude larger than our prediction based on SU(3) breaking. This would then seem to represent fairly strong evidence for the existence of a second-class interaction in the weak Hamiltonian. It should also be noted that the values for f_1, f_2, and g_1 in (5.3) also differ considerably from the Cabibbo values. Thus the entire fit (5.3) is in strong disagreement with the Cabibbo theory.

Since 1971 the CERN group has obtained a value for the neutrino asymmetry,[6] and the Argonne group has analyzed the rest of its data.[4] The new CERN value is $\alpha_\nu = 0.89 \pm 0.08$, which is considerably higher than the value $\alpha_\nu = 0.74 \pm 0.16$ used by Garcia and is almost within one standard deviation of the Cabibbo prediction $\alpha_\nu = 0.98$. Using the CERN results for the asymmetries together with the world average for the $\Lambda \to p$ decay rate,[44] we find that the two types of solution observed by Garcia are still present. With $g_2 = 0$ there is a solution close to the Cabibbo values; with $g_2 \neq 0$ there is a solution differing considerably from the Cabibbo values. But the relative probabilities for the two solutions are now quite different from those found by Garcia.[52] Thus the χ^2 of the Cabibbo ($g_2 = 0$) solution is 2.30, corresponding to a probability of 32%. For the non-Cabibbo ($g_2 \neq 0$) solution, χ^2 is reduced to 1.22, but with one less degree of freedom the probability is actually slightly lower, 28%. Thus the $g_2 = 0$ solution is the preferred one for the CERN data. Furthermore, the CERN group[6] has made a fit to the proton recoil spectrum and to the three spin asymmetries in their statistically-independent combinations $(\alpha_e + \alpha_\nu)$, $(\alpha_\nu + \alpha_p)$, and $(\alpha_p + \alpha_e)$. With $g_2 = 0$ assumed, they find a very good fit (76% probability) in terms of g_1/f_1 and f_2/f_1. The values obtained,

$$g_1/f_1 = 0.63 \pm 0.06, \quad f_2/f_1 = 1.5 \pm 1.7, \tag{5.4}$$

are consistent with the Cabibbo predictions. Thus the CERN experiment appears to be well described by the Cabibbo theory without an additional large pseudotensor term.

The result of the complete Argonne analysis for the neutrino asymmetry is $\alpha_\nu = 0.71 \pm 0.10$.[53] This is nearly the same value (with a smaller error) as that used by Garcia. Furthermore, the Argonne values for the other asymmetry parameters agree quite closely with those in the original Garcia analysis. Thus the Argonne results favor a solution with a large pseudotensor form factor, like that in (5.3).

The experimental situation regarding $g_2(0)$ for the $\Lambda \to p$ decay thus appears to be contradictory.

The CERN experiment favors a zero or small value, which is consistent with our estimate based on SU(3) breaking. The Argonne experiment, on the other hand, favors a very large value and thus seems to suggest the presence of a second-class term in the weak Hamiltonian. It is clearly of great interest to resolve this experimental discrepancy. It should be noted, however, that the values obtained in the CERN and Argonne experiments for the asymmetry parameters are not inconsistent with each other. So perhaps one should view the discrepancy for $g_2(0)$ with some caution.

It would be quite difficult to observe the pseudotensor term in the decay $\Sigma^- \to n + e^- + \bar{\nu}_e$. In order to determine both $g_1(0)$ and $g_2(0)$ [in addition to $f_1(0)$], one would have to produce polarized Σ^- hyperons and detect the final neutron. While experiments have been performed incorporating one or the other of these features,[54] no attempt has been made to combine them in a single experiment. More promising are the decays $\Sigma^\pm \to \Lambda + e^\pm \pm \nu_e$. Here the Λ decay permits a complete kinematic analysis of the three-body final state and also is a good analyzer of the Λ polarization. For $\Sigma^\pm \to \Lambda$ the conserved-vector-current (CVC) hypothesis implies that $f_1(0) = 0$ in the symmetry limit. By the Ademollo-Gatto theorem[40] the corrections to $f_1(0)$ are expected to be of second order in the symmetry breaking. Thus $f_1(0) \sim O(\alpha)$ and so is expected to be negligible. One could then fit the decay data in terms of $g_1(0)$, $f_2(0)$, and $g_2(0)$. From Eq. (5.1) we see that $g_2(0)$ may be fairly large for these decays even if there is no direct second-class coupling. A somewhat different philosophy has been applied to the experimental analysis of the $\Sigma^\pm \to \Lambda$ decays.[55] $g_2(0)$ was kept equal to zero, and deviations from the CVC prediction $f_1(0) = 0$ were sought. The value obtained was $f_1(0)/g_1(0) = -0.37 \pm 0.20$. While this result may be consistent with zero as stated in Ref. 55, the actual numerical value of 0.37 is clearly much greater than would be expected from a second-order electromagnetic effect. From a theoretical standpoint it is thus important to see whether a better fit could be obtained by allowing $g_2(0)$ to vary while keeping $f_1(0) = 0$. In this regard it should be recalled that SU(3) breaking leads to values of $g_2(0)/g_1(0)$ that are the same for $\Sigma^+ \to \Lambda$ and $\Sigma^- \to \Lambda$, while a direct second-class coupling leads [in the SU(3) limit] to opposite values for the two decays.[56] In Ref. 55 an upper limit $|g_2(0)/g_1(0)| < 6.2$ was obtained for a pseudotensor term with opposite sign, but no estimate was made for a term with the same sign. Because of this ability to distinguish between genuine second-class effects and SU(3)-symmetry-breaking effects, the $\Sigma^\pm \to \Lambda$ decays probably provide the best opportunity in particle physics to determine unambiguously whether second-class currents are present in weak interactions.

APPENDIX A: THE AXIAL-VECTOR-CURRENT-VECTOR-PSEUDOSCALAR VERTEX

This appendix is devoted to determining the matrix element of the strangeness-changing axial-vector current between vector- and pseudoscalar-meson states by means of PCAC and hard-pion techniques. In particular, we shall consider the matrix element $\langle \pi | A_\mu^{(\Delta S=1)} | K^* \rangle$, which can be related to experimental information, and then assume SU(3) symmetry for the other meson states. The general form of the matrix element is thus

$$(4\omega_M \omega_V \Omega^2)^{1/2} \langle M^k(k) | \sin\theta_C A_\mu^{(\Delta S=1)i}(0) | V^j(p) \rangle = \sin\theta_C f_{ijk} [\epsilon_\mu F_1(q^2) + p_\mu (\epsilon \cdot q) F_2(q^2) + q_\mu (\epsilon \cdot q) F_3(q^2)], \tag{A1}$$

where $q \equiv p - k$. Note that a symmetric (d_{ijk}) coupling would constitute a direct second-class contribution to the axial current.[30,31] For the present calculation we need to determine only F_1 and F_2. Using standard reduction techniques and the assumption of PCAC,

$$\partial_\mu A_\mu^i(x) = F_\pi m_\pi^2 \phi_\pi^i(x), \tag{A2}$$

where $F_\pi \approx 92$ MeV, we can write the matrix element in (A1) as[57]

$$-\sin\theta_C \epsilon_\nu^{K^*}(p) \frac{(k^2 + m_\pi^2)(p^2 + m_{K^*}^2)}{F_\pi m_\pi^2 g_{K^*}} \int d^4x\, d^4y\, e^{-ik\cdot x} e^{-iq\cdot y} \langle 0 | T\{\partial_\lambda A_\lambda^k(x) A_\mu^i(y) V_\nu^j(0)\} | 0 \rangle . \tag{A3}$$

We exhibit the pole structure of the T product in terms of the $K^*K\pi$ vertex $\Gamma_\mu(k, q)$ and the $K_A K^*\pi$ vertex $\Gamma_{\mu\nu}(k, q)$ by the following definition:

$$\int d^4x\, d^4y\, e^{-ik\cdot x} e^{-iq\cdot y}\langle 0|\, T\{\partial_\lambda A_\lambda^k(x) A_\mu^i(y) V_\nu^j(0)\}|0\rangle \equiv f_{ijk}\frac{F_\pi m_\pi^2}{g_{K^*} g_{K_A}(k^2+m_\pi^2)}\,\Delta_{\mu\sigma}^{K_A}(q)\Delta_{\nu\eta}^{K^*}(p)\Gamma_{\sigma\eta}(k,q)$$

$$-f_{ijk}\frac{F_\pi F_K m_\pi^2}{g_{K^*}(k^2+m_\pi^2)(q^2+m_K^2)}\,q_\mu \Delta_{\nu\eta}^{K^*}(p)\Gamma_\eta(k,q)\,. \qquad \text{(A4)}$$

$\Delta_{\mu\nu}^{K^*}(p)$ and $\Delta_{\mu\nu}^{K_A}(q)$ are the covariant spin-1 parts of the unrenormalized vector and axial-vector propagators. With the assumption of single-particle dominance for these propagators and using Eq. (A4) and the result $\epsilon^{K^*}(p)\cdot p = 0$, we can write Eq. (A3) as

$$-\sin\theta_C f_{ijk}\left[\frac{g_{K_A}}{(q^2+m_{K_A}^2)}\right]\epsilon_\eta^{K^*}(p)[\delta_{\mu\sigma}+q_\mu q_\sigma/m_{K_A}^2]\Gamma_{\sigma\eta}(k,q)+\sin\theta_C f_{ijk}[F_K/(q^2+m_K^2)]\epsilon_\eta(p)q_\mu\Gamma_\eta(k,q)\,. \qquad \text{(A5)}$$

The terms proportional to q_μ contribute only to F_3, and so we neglect them. Thus we have

$$(4\omega_M\omega_V\Omega^2)^{1/2}\langle M^K(k)|\sin\theta_C\, A_\mu^{(\Delta S=1)\,i}(0)|\, V^j(p)\rangle \doteq -\sin\theta_C f_{ijk}[g_{K_A}/(q^2+m_{K_A}^2)]\epsilon_\eta^{K^*}(p)\Gamma_{\mu\eta}(k,q)\,, \qquad \text{(A6)}$$

where $\doteq$ indicates that we retain only the terms of interest. In the limit $q^2\to 0$ we then find

$$\epsilon_\mu^{K^*}(p)F_1(0)+p_\mu\epsilon^{K^*}(p)\cdot qF_2(0)\doteq -(g_{K_A}/m_{K_A}^2)\epsilon_\eta^{K^*}(p)\Gamma_{\mu\eta}(k,q)\,. \qquad \text{(A7)}$$

We thus need to determine the $K_A K^*\pi$ vertex $\Gamma_{\mu\nu}$. Gerstein and Schnitzer[29] have obtained an explicit expression for this vertex by assuming that single particles dominate all propagators, that the primitive three-point functions are slowly varying functions of momenta, and that the chiral-symmetry-breaking term in the Lagrangian transforms as $(3,\bar{3})\oplus(\bar{3},3)$. From Eqs. (A15) and (A16) of their paper we find (in our notation)

$$\begin{aligned}\epsilon_\eta^{K^*}(p)\Gamma_{\mu\eta}(k,q) &= -(C_{A_1}/F_\pi g_{A_1})\epsilon_\eta^{K^*}(p)k_\sigma\Gamma_{\sigma\mu\eta}(k,q)-(g_{K_A}g_{K^*}/F_\pi)\epsilon_\eta^{K^*}(p)\Delta_{K_A}^{-1}{}_{\mu\eta}(q)\\ &= -[C_{A_1}m_{K^*}{}^2/F_\pi g_{K^*}g_{A_1}]\epsilon_\eta^{K^*}(p)\{-2g_1k_\mu q_\eta+g_2[q_\eta(p+k)_\mu+\delta_{\mu\eta}k\cdot(p+q)]+g_3(q_\eta p_\mu+\delta_{\mu\eta}k\cdot p)\\ &\qquad +g_5[q_\eta(p+k)_\mu-\delta_{\mu\eta}k\cdot(p+q)]+g_6(q_\eta p_\mu-\delta_{\mu\eta}k\cdot p)\}\\ &\quad -(g_{K^*}/F_\pi g_{K_A})\epsilon_\eta^{K^*}(p)[(q^2+m_{K_A}^2)\delta_{\mu\eta}-q_\mu q_\nu]\,. \end{aligned} \qquad \text{(A8)}$$

$g_1,\ldots,g_6$ are unknown parameters. The smoothness assumption requires that $g_1=g_2$ and $g_4=g_6=-g_5$. We again neglect terms proportional to q_μ, and so we have

$$\begin{aligned}\epsilon_\eta^{K^*}(p)\Gamma_{\mu\eta}(k,q)\doteq &-[C_{A_1}m_{K^*}{}^2/F_\pi g_{K^*}g_{A_1}]\{\epsilon_\mu^{K^*}(p)[g_2k\cdot(p+q)+g_3k\cdot p-g_5k\cdot q]+\epsilon^{K^*}(p)\cdot q p_\mu(g_3+g_5)\}\\ &-(g_{K^*}/F_\pi g_{K_A})(q^2+m_{K_A}^2)\epsilon_\mu^{K^*}(p)\,. \end{aligned} \qquad \text{(A9)}$$

Evaluating Eq. (A9) at $q^2=0$, using $C_{A_1}=g_{A_1}{}^2/m_{A_1}{}^2$, and comparing with Eq. (A7), we find

$$F_1(0)=-[\,g_{K_A}g_{A_1}m_{K^*}{}^2/F_\pi g_{K^*}m_{K_A}{}^2m_{A_1}{}^2][g_2m_{K^*}{}^2+\tfrac{1}{2}g_3(m_{K^*}{}^2+m_\pi{}^2)-\tfrac{1}{2}g_5(m_{K^*}{}^2-m_\pi{}^2)]+g_{K^*}/F_\pi\,, \qquad \text{(A10)}$$

$$F_2(0)=(g_{K_A}g_{A_1}m_{K^*}{}^2/F_\pi g_{K^*}m_{K_A}{}^2m_{A_1}{}^2)(g_3+g_5)\,. \qquad \text{(A11)}$$

Unfortunately, it is not possible to determine the parameters g_2, g_3, and g_5 (as well as g_{K_A} and g_{K^*}) reliably. The indications are, however, that the deviations from exact SU(3) symmetry are small.[29] In this limit

$$g_2=1,\quad g_3=\delta_{K^*},\quad g_5=0\,, \qquad \text{(A12)}$$

where δ_{K^*} is still unknown. We shall assume these values. Furthermore, we use Weinberg's first sum rules,[58] the KSRF (Kawarabayashi-Suzuki-Riazuddin-Fayyazuddin) relation,[59] $F_K{}^2\approx F_\pi{}^2$, and $F_\kappa{}^2\ll F_\pi{}^2$ (see Ref. 29) to derive

$$g_{K_A}{}^2/m_{K_A}{}^2\approx g_{A_1}{}^2/m_{A_1}{}^2\approx g_{K^*}{}^2/2m_{K^*}{}^2\approx F_\pi{}^2\,. \qquad \text{(A13)}$$

With these approximations $F_1(0)$ and $F_2(0)$ depend on the single parameter δ_{K^*}.

$$F_1(0) = -(m_{K^*}/\sqrt{2}m_{K_A}m_{A_1})[m_{K^*}^2 + \tfrac{1}{2}\delta_{K^*}(m_{K^*}^2 + m_\pi^2)] + \sqrt{2}m_{K^*}, \tag{A14}$$

$$F_2(0) = (m_{K^*}/\sqrt{2}m_{K_A}m_{A_1})\delta_{K^*}. \tag{A15}$$

The sign conventions used in deriving (A14) and (A15) are discussed below.

To determine δ_{K^*}, we consider the decays $K_A \to K^*\pi$ and $K^* \to K\pi$.[60] The on-shell $K_A K^*\pi$ vertex is given by

$$\begin{aligned} -f_{ijk}\epsilon_\mu^{K_A}(q)\epsilon_\eta^{K^*}(p)\Gamma_{\mu\eta}(k,q) = f_{ijk}\epsilon_\mu^{K_A}(q)\epsilon_\eta^{K^*}(p)[g_{A_1}m_{K^*}^2/F_\pi g_{K^*}m_{A_1}^2] \\ \times\{[g_2(m_{K_A}^2 - m_{K^*}^2) + \tfrac{1}{2}g_3(m_{K_A}^2 - m_{K^*}^2 - m_\pi^2) \\ -\tfrac{1}{2}g_5(m_{K_A}^2 - m_{K^*}^2 + m_\pi^2)]\delta_{\mu\eta} + (g_3 + g_5)p_\mu q_\eta\}. \end{aligned} \tag{A16}$$

With the approximations (A12) and (A13) we then find that the $K_A K^*\pi$ coupling constants are given by

$$\mathfrak{F}_1 = (m_{K^*}/\sqrt{2}F_\pi m_{A_1})[m_{K_A}^2 - m_{K^*}^2 + \tfrac{1}{2}\delta_{K^*}(m_{K_A}^2 - m_{K^*}^2 - m_\pi^2)], \tag{A17}$$

$$\mathfrak{F}_2 = (m_{K^*}/\sqrt{2}F_\pi m_{A_1})\delta_{K^*}. \tag{A18}$$

The width for the decay $K_A \to K^*\pi$ is given in terms of $\mathfrak{F}_1$ and $\mathfrak{F}_2$ by

$$\Gamma(K_A \to K^*\pi) = (k/32m_{K_A}^2)[(3 + k^2/m_{K^*}^2)\mathfrak{F}_1^2 - 2k^2(m_{K_A}E_{K^*}/m_{K^*}^2)\mathfrak{F}_1\mathfrak{F}_2 + k^4(m_{K_A}^2/m_{K^*}^2)\mathfrak{F}_2^2], \tag{A19}$$

where k is the decay three-momentum in the K_A rest frame. The width for the decay $K^* \to K\pi$ can also be related to the parameter δ_{K^*},

$$\Gamma(K^* \to K\pi) = (k^3/16\pi F_\pi^2) \times [1 - m_{K^*}^2(1 + \delta_{K^*})/2m_{K_A}m_{A_1}]^2. \tag{A20}$$

In Table VIII the decay widths and form factors are tabulated as a function of δ_{K^*}. The following mass values have been used: $m_{K^*} = 892.6$ MeV, $m_{A_1} = 1070$ MeV, and $m_{K_A} = 1243$ MeV (see Ref. 44). The experimental values for the widths are $\Gamma(K^* \to K\pi) = (50.1 \pm 1.1)$ MeV (see Ref. 44), and $\Gamma(K_A \to K^*\pi) = (70^{+26}_{-18})$ MeV (see Ref. 48). Thus we see that $\delta_{K^*} \cong -0.8$. We shall then use the following values for $F_1(0)$ and $F_2(0)$:

$$F_1(0) \cong 1.0 \text{ GeV}, \quad F_2(0) \cong -0.4 \text{ GeV}^{-1}. \tag{A21}$$

TABLE VIII. Decay widths and form factors as a function of the parameter δ_{K^*}.

δ_{K^*}	$\Gamma(K^* \to K\pi)$ (MeV)	$\Gamma(K_A \to K^*\pi)$ (MeV)	$\mathfrak{F}_1$ (GeV)	$\mathfrak{F}_2$ (GeV^{-1})	$F_1(0)$ (GeV)	$F_2(0)$ (GeV^{-1})
0.0	27.5	126.6	4.80	0.00	0.88	0.00
−0.1	29.9	115.7	4.56	−0.64	0.90	−0.05
−0.2	32.4	105.3	4.33	−1.28	0.92	−0.10
−0.3	35.0	95.5	4.10	−1.92	0.94	−0.14
−0.4	37.7	86.1	3.86	−2.56	0.96	−0.19
−0.5	40.5	77.2	3.63	−3.21	0.98	−0.24
−0.6	43.4	68.8	3.39	−3.85	1.00	−0.29
−0.7	46.4	61.0	3.16	−4.49	1.02	−0.33
−0.8	49.5	53.6	2.93	−5.13	1.04	−0.38
−0.9	52.7	46.7	2.69	−5.77	1.06	−0.43
−1.0	56.0	40.3	2.46	−6.41	1.08	−0.48

It is interesting to compare the present results with those obtained in the soft-pion limit and with the assumption of K_A dominance for the form factors,

$$\begin{aligned} \mathfrak{F}_1^{(\pi\to 0)} &\cong \sqrt{2}m_{K^*}(m_{K_A}^2 - m_{K^*}^2)/F_\pi m_{K_A} \\ &= 8.24 \text{ GeV}, \\ F_1^{(\pi\to 0)}(0) &\cong \sqrt{2}m_{K^*}(m_{K_A}^2 - m_{K^*}^2)/m_{K_A}^2 \\ &= 0.61 \text{ GeV}. \end{aligned}$$

Thus while the soft-pion result for $F_1(0)$ is not unreasonable, that for $\mathfrak{F}_1$ is nearly a factor of three too large. As a consequence, it is not possible to determine a value for $\mathfrak{F}_2$ from Eq. (A19) using the experimental $K_A \to K^*\pi$ width and the soft-pion value for $\mathfrak{F}_1$ as input.

We now return to the question of the choice of signs used in obtaining (A14) and (A15) from (A10)–(A13). With our conventions, the Goldberger-Treiman relation[61] has the form

$$F_\pi g_{\pi NN} = m_N g_1^{(N)}, \tag{A22}$$

where $g_1^{(N)} = +(1.24)\cos\theta_C$ is the axial-vector form factor in neutron beta decay. We thus conclude that $F_\pi g_{\pi NN}$ is positive. The contribution of the triangle graph is proportional to $g_{\pi NN}G_{1,2}F_{1,2}$. We recall from Eq. (3.5) that the sign of $G_{1,2}$ is determined by that of $\hat{\gamma}_\rho$, which in the present no-

tation is $m_\rho^2/2g_\rho$. Thus from Eqs. (A10) and (A11) we see that the over-all sign of the triangle graph is determined by the signs of

$$g_{K_A} g_{A_1} g_{\pi NN}/F_\pi g_\rho g_{K^*}, \tag{A23}$$

and

$$g_{\pi NN} g_{K^*}/F_\pi g_\rho . \tag{A24}$$

Since we expect SU(3)-symmetry breaking to be small, we assume that g_ρ and g_{K^*} have the same sign and that g_{A_1} and g_{K_A} have the same sign. It then follows that both (A23) and (A24) are positive. For definiteness we shall take g_{K_A}, g_{A_1}, $g_{\pi NN}$, F_π, g_ρ, and g_{K^*} all to be positive.

For the $\Sigma^\pm \to \Lambda$ decays we need the matrix element of the strangeness-conserving axial current between meson states. The general form of this matrix element will be the same as in Eq. (A1) but with $\sin\theta_C$ replaced by $\cos\theta_C$. The form factors $F_1(q^2)$ and $F_2(q^2)$ can be determined from the hard-pion, chiral SU(2)⊗SU(2) calculation of Schnitzer and Weinberg.[62] The results are identical to Eqs. (A14)–(A15) and (A17)–(A18) but with the replacements $m_{K^*} \to m_\rho$, $m_{K_A} \to m_{A_1}$, and $\delta_{K^*} \to \delta_{\rho\pi}$. Using the $\rho \to \pi\pi$ width to determine $\delta_{\rho\pi}$, one obtains the same values (to within 10%) for $F_1(0)$ and $F_2(0)$ as those in (A21). Thus to a good approximation we can take advantage of the SU(3)-symmetric form of the coupling (A1) and employ it for all the components of the axial-vector current.

APPENDIX B: TRIANGLE DIAGRAM CONTRIBUTION TO $g_2(q^2)$

If one evaluates the graphs in Fig. 2 according to the usual Feynman rules employing the couplings of Eqs. (3.1), (3.2), and (3.8), then the induced pseudotensor form factor extracted from these graphs has the form

$$g_2^{(a,b)}(q^2) = -g_{\pi NN} A_{VMB}^{1,2} (16\pi^2)^{-1} 2 \left\{ \int_0^\infty k^2 dk^2 \int_0^1 dx \int_0^x dy \, [H_1^{(a,b)}(x,y,q^2) + k^2 H_2^{(a,b)}(x,y,q^2)] \right.$$
$$\times [k^2 + q^2 y(x-y) + \alpha^{(a,b)}(x) y + \beta^{(a,b)}(x)]^{-3}$$
$$\left. + \int_0^1 dx \int_0^x dy \, S^{(a,b)}(x,y,q^2) \right\} (m_1 + m_2). \tag{B1}$$

All the SU(3) dependence of the graphs has been absorbed into the term $A_{VMB}^{1,2}$. The functions $\alpha^{(a,b)}(x)$ and $\beta^{(a,b)}(x)$ depend on the masses of the particles:

$$\alpha^{(a)}(x) = (m_1^2 - m_2^2)(1-x) + \mu_M^2 - \mu_V^2, \tag{B2}$$
$$\alpha^{(b)}(x) = (m_1^2 - m_2^2)(1-x) + \mu_V^2 - \mu_M^2, \tag{B3}$$
$$\beta^{(a)}(x) = m_1^2 x^2 + (\mu_V^2 - m_1^2 - m^2)x + m^2, \tag{B4}$$
$$\beta^{(b)}(x) = m_1^2 x^2 + (\mu_M^2 - m_1^2 - m^2)x + m^2 . \tag{B5}$$

The functions H_1, H_2, and S depend on four products of coupling constants: F_1G_1, F_1G_2, F_2G_1, and F_2G_2. The coupling F_3 [see Eq. (3.8)] does not contribute to $g_2(q^2)$. The explicit expressions for these functions are as follows:

$$H_1^{(a)}(x,y,q^2) = F_1G_1\{x - y + (1-x)(2\mu_V^2)^{-1}\{-m_1(1-x)(m+m_1x) + y(m_1+m_2)[m_1 - m + (m_2 - m_1)x] + q^2 y(x-y)\}\}$$
$$+ F_1G_2(m_1+m)^{-1}\{\tfrac{1}{2}(1-x)(m_1x - m) + y[\tfrac{1}{2}(m_2 - m_1)(1-x) - (m - m_2x)]\}$$
$$+ F_2G_1\tfrac{1}{2}(1-x)[(m_1+m_2)(m-m_2x) - q^2(x-y) + (2\mu_V^2)^{-1}$$
$$\times ((m_1^2 - m_2^2 - q^2)(1-x)\{-m_1(1-x)(m+m_1x) + y(m_1+m_2)[m_1 - m + (m_2 - m_1)x]\}$$
$$+ q^2 y\{(1-x)[2m_1m + (3m_1^2 - m_2^2)x] + y(m_1+m_2)[2m - 3m_1 + m_2 + 3x(m_1 - m_2)]\}$$
$$- q^4 y(x-y)(1 - x + 2y))]$$
$$+ F_2G_2\tfrac{1}{4}(1-x)^2(m_1+m)^{-1}\{(m_1^2 - m_2^2 - q^2)[m_1x - m + y(m_2 - m_1)] - 2m_1^2(m_1+m_2)(x-y)\}, \tag{B6}$$

$$H_1^{(b)}(x,y,q^2) = F_1G_1\{-y+(1-x)(2\mu_V^2)^{-1}[m_2m+m_1(m-m_2)x-m_1^2x^2+y(m_1+m_2)[m_2-m-(m_2-m_1)x] - q^2y(x-y)]\}$$
$$+F_1G_2(m_2+m)^{-1}\{\tfrac{1}{2}(1+x)(m-m_1x)+y[\tfrac{1}{2}(m_1-m_2)(1-x)-m+m_1x]\}$$
$$+F_2G_1\tfrac{1}{2}(1-x)[(m_1+m_2)(m_1x-m)+q^2y$$
$$+(2\mu_V^2)^{-1}([(m_1^2-m_2^2)(1-x)+q^2(1+x)]\{-m_2m-m_1(m-m_2)x+m_1^2x^2$$
$$+y(m_1+m_2)[m-m_2+(m_2-m_1)x]\}$$
$$+q^2y\{2m_2m+2m_1(m-m_2)x-2m_1^2x^2+y(m_1+m_2)[3m_2-2m-m_1+3x(m_1-m_2)]\}$$
$$-q^4y(x-y)(-1-x+2y))]$$
$$+F_2G_2\tfrac{1}{4}(x-1)(m_2+m)^{-1}\{[(m_1^2-m_2^2)(1+x)+q^2(1-x)][m-m_1x+y(m_1-m_2)]$$
$$+2m_2(m_1+m_2)(m_1x-m_2)\}, \tag{B7}$$

$$H_2^{(a)}(x,y,q^2) = F_1G_1(-(1-\tfrac{3}{2}x)(2\mu_V^2)^{-1})+F_1G_2(0)$$
$$+F_2G_1\tfrac{1}{4}\{-1+(\mu_V^2)^{-1}[(m_1^2-m_2^2-q^2)(-1+3x-2x^2)+\tfrac{1}{2}(m-m_1)(m_1+m_2)(1-x)+yq^2(3-4x)]\}$$
$$+F_2G_2(-\tfrac{1}{4})(m_1+m)^{-1}[m+\tfrac{5}{2}m_1(1-x)+\tfrac{3}{2}m_2-\tfrac{5}{2}m_2x], \tag{B8}$$

$$H_2^{(b)}(x,y,q^2) = F_1G_1((1-\tfrac{3}{2}x)(2\mu_V^2)^{-1})+F_1G_2(0)$$
$$+F_2G_1\tfrac{1}{4}\{1+(\mu_V^2)^{-1}[(m_1^2-m_2^2)(-1+3x-2x^2)-\tfrac{1}{2}(m-m_2)(m_1+m_2)(1-x)$$
$$-q^2(1-2x^2)+yq^2(3-4x)]\}+F_2G_2\tfrac{1}{4}(m_2+m)^{-1}[m+\tfrac{3}{2}m_1-\tfrac{5}{2}m_1x+\tfrac{5}{2}m_2(1-x)], \tag{B9}$$

$$S^{(a)}(x,y,q^2) = F_1G_1(-x/4\mu_V^2)+F_1G_2(0)$$
$$+F_2G_1(12\mu_V^2)^{-1}[\tfrac{1}{2}x(7x-6)(m_1^2-m_2^2-q^2)-\tfrac{1}{2}x(m_1-m)(m_1+m_2)+yq^2(7x-3)]$$
$$+F_2G_2(m_1+m)^{-1}[-5(m_1+m_2)x/24], \tag{B10}$$

$$S^{(b)}(x,y,q^2) = F_1G_1(x/4\mu_V^2)+F_1G_2(0)$$
$$+F_2G_1(12\mu_V^2)^{-1}[\tfrac{1}{2}x(m_1^2-m_2^2)(7x-6)-\tfrac{7}{2}x^2q^2+\tfrac{1}{2}x(m_2-m)(m_1+m_2)+yq^2(7x-3)]$$
$$+F_2G_2(m_2+m)^{-1}[5(m_1+m_2)x/24]. \tag{B11}$$

The explicit forms for $S^{(a,b)}$ depend on the choice of momentum variable in the triangle graph. The expressions given above in (B10) and (B11) are obtained with the baryon carrying the loop momentum. Since the surface terms do not contribute to the discontinuity, the *dispersion* evaluation of $g_2(q^2)$ is free of any ambiguity arising from the choice of routing of momentum in the diagram.

---

*Research supported in part by the National Science Foundation.

†Present Address: Center for Particle Theory, University of Texas, Austin, Texas 78712

[1]N. Cabibbo, Phys. Rev. Lett. 10, 531 (1963).

[2]M. Roos, Phys. Lett. 36B, 130 (1971).

[3]J. Lindquist, R. L. Sumner, J. M. Watson, R. Winston, D. M. Wolfe, P. R. Phillips, E. C. Swallow, K. Reibel, D. M. Schwartz, A. J. Stevens, and T. A. Romanowski, Phys. Rev. Lett. 27, 612 (1971).

[4]J. Lindquist *et al.*, Paper No. 457 presented at the Sixteenth International Conference on High Energy Physics, University of Chicago and National Accelerator Laboratory, Batavia, Ill., 1972.

[5]K. H. Althoff, R. M. Brown, D. Freytag, K. S. Heard, J. Heintze, R. Mundhenke, H. Rieseberg, V. Soergel, H. Stelzer, and A. Wagner, Phys. Lett. 37B, 531 (1971); 37B, 535 (1971).

[6]K. H. Althoff *et al.*, Phys. Lett. 43B, 237 (1973).

[7]Augusto Garcia, Phys. Rev. D 3, 2638 (1971).

[8]A preliminary account of this work for the decay $\Lambda \to p + e^- + \bar{\nu}_e$ has been published previously. See P. L. Pritchett and N. G. Deshpande, Phys. Lett. 41B, 311 (1972).

[9]We use a metric such that $a_\mu = (\vec{a}, ia_0)$. Our γ matrices are Hermitian and satisfy $\gamma_\mu\gamma_\nu + \gamma_\nu\gamma_\mu = 2\delta_{\mu\nu}$. The Dirac equation is $(i\gamma\cdot p + m)u(p) = 0$, and the spinors are normalized to $\bar{u}u = 1$. We set $\hbar = c = 1$ and have $\alpha = e^2/4\pi \approx \frac{1}{137}$. In this metric $\gamma_5 = \gamma_1\gamma_2\gamma_3\gamma_4$.

[10]With the present conventions $g_1(0)/f_1(0)$ is positive for neutron beta decay.

[11]S. Weinberg, Phys. Rev. 112, 1375 (1958).

[12]L. Wolfenstein, Phys. Rev. 135, B1436 (1964).

[13]The vanishing of f_3 and g_2 can also be deduced from the alternative assumptions of time-reversal invariance and the charge symmetry condition for the current, $e^{-i\pi T_2} J_\mu^{(+)}(x) e^{i\pi T_2} = -J_\mu^{(-)}(x)$. Furthermore, if the vector part of J_μ is conserved, then f_3 will vanish regardless of the first- or second-class nature of J_μ.

[14]See the very clear discussion of this point given by R. Gatto, in *Symmetries in Elementary Particles*, edited by A. Zichichi (Academic, New York, 1965), p. 175.

[15]The relative sign depends on phase conventions for the states. With the Condon and Shortley convention, the matrix elements will be related by a minus sign.

[16]Hans A. Bethe and Frederic de Hoffmann, *Mesons and Fields* (Row, Peterson and Company, Evanston, Ill., 1955), Vol. II.

[17]G. F. Chew, R. Karplus, S. Gasiorowicz, and F. Zachariasen, Phys. Rev. 110, 265 (1958).

[18]P. Federbush, M. L. Goldberger, and S. B. Treiman, Phys. Rev. 112, 642 (1958).

[19]In Ref. 16 the statement is made that "if diagrams a and b are added—but not if they are treated separately—renormalization is unnecessary because the result converges even in the old-fashioned perturbation theory." This is incorrect. The contributions to the anomalous moment from (a) and (b) separately are finite without renormalization. Indeed, it is clear from Eq. (2.1) that if they were not it would be impossible for both λ_p and λ_n to be finite.

[20]K. Nakabayasi and I. Sato, Prog. Theor. Phys. 6, 252 (1951); K. Nakabayasi, I. Sato, and T. Akiba, *ibid.* 12, 250 (1954).

[21]W. R. Frazer and J. R. Fulco, Phys. Rev. Lett. 2, 365 (1959); Phys. Rev. 117, 1609 (1960).

[22]W. R. Frazer and J. R. Fulco, Phys. Rev. 117, 1603 (1960).

[23]A. Erwin, R. March, W. Walker, and E. West, Phys. Rev. Lett. 6, 628 (1961).

[24]D. Benaksas, G. Cosme, B. Jean-Marie, S. Jullian, F. Laplanche, J. Lefrançois, A. D. Liberman, G. Parrour, J. P. Repellin, and G. Sauvage, Phys. Lett. 39B, 289 (1972).

[25]V. Singh and B. M. Udganokar, Phys. Rev. 128, 1820 (1962).

[26]J. S. Ball and D. Y. Wong, Phys. Rev. 130, 2112 (1963).

[27]In Ref. 8, SU(3) symmetry was assumed for the dimensional coupling $G_2/2m_N$. The present modification leads to only minor changes in the results of Ref. 8.

[28]H. J. Schnitzer and S. Weinberg, Phys. Rev. 164, 1828 (1967).

[29]I. S. Gerstein and H. J. Schnitzer, Phys. Rev. 175, 1876 (1968).

[30]H. J. Lipkin, Phys. Rev. Lett. 27, 432 (1971).

[31]H. Pietschmann and H. Rupertsberger, Phys. Lett. 40B, 662 (1972).

[32]Throughout the calculation we shall consistently ignore electromagnetic mass differences and simply use the mean mass value in each isotopic multiplet.

[33]J. M. Jauch and F. Rohrlich, *The Theory of Photons and Electrons* (Addison-Wesley, Reading, Mass., 1955), Appendix A5-2. Note that the value of the surface terms depends on the routing of the loop momentum in the triangle graph. See the discussion in Appendix B.

[34]M. Jacob and G. C. Wick, Ann. Phys. (N.Y.) 7, 404 (1959).

[35]We use the angular momentum notation of A. R. Edmonds, *Angular Momentum in Quantum Mechanics*, (Princeton Univ. Press, Princeton, New Jersey, 1960), 2nd edition.

[36]For the case of $N\bar{N} \to \pi\pi$ annihilation, the violation of unitarity above threshold due to use of the Born approximation was equally rapid and severe.

[37]Here only the isospin-$\frac{1}{2}$ part of the amplitude is considered.

[38]In the numerical calculations of $g_2(0)$ all integrals were done analytically except for the final integration over the parameter x [cf. Eq. (3.21)], which was performed numerically.

[39]The numerical values presented in Ref. 8 were obtained by a still different procedure. The Feynman evaluation was performed for those terms contributing to the discontinuity in q^2 but with a cutoff corresponding to a dispersion mass $\sigma^2 = \Lambda^2$. While the final value for $g_2(0)$ was nearly the same as the present result, the contributions from individual states for a given Λ^2 were considerably smaller. (Compare Table I in Ref. 8 with the present Table IV.) We feel that the present dispersion evaluation is the more reasonable one.

[40]M. Ademollo and R. Gatto, Phys. Rev. Lett. 13, 264 (1964).

[41]In evaluating the sum rules (3.37) and (3.38), we divide out factors of $\sin\theta_C$ and $\cos\theta_C$ from $g_2(0)$ since the sum rules refer to octets of vector and axial-vector currents rather than the Cabibbo current.

[42]H. Pilkuhn, in *Springer Tracts in Modern Physics*, edited by G. Hoehler (Springer, Berlin, Germany, 1970), Vol. 55, p. 168.

[43]Values quoted by G. Wolf, in *Proceedings of the 1971 International Symposium on Electron and Photon Interactions at High Energies*, edited by N. B. Mistry (Cornell Univ. Press, Ithaca, New York, 1972), p. 189.

[44]Particle Data Group, Phys. Lett. 39B, 1 (1972).

[45]C. López and F. J. Yndurâin, Phys. Lett. 41B, 183 (1972).

[46]J. Engels and H. Pilkuhn, Nucl. Phys. B31, 531 (1971).

[47]R. C. Chase, E. Coleman, H. W. Courant, E. Marquit, E. W. Petraske, H. F. Romer, and K. Ruddick, Phys. Lett. 30B, 659 (1969).

[48]A. F. Garfinkel, R. F. Holland, D. D. Carmony, H. W. Clopp, D. Cords, F. J. Loeffler, L. K. Rangan, R. L. Lander, D. E. Pellett, and P. M. Yager, Phys. Rev. Lett. 26, 1505 (1971).

[49]B. Renner, Phys. Lett. 33B, 599 (1970).

[50]J. Engels, Nucl. Phys. B25, 141 (1971); R. Aaron and H. Goldberg, Phys. Rev. D 6, 2704 (1972).

[51]J. Rosner, C. Rebbi, and R. Slansky, Phys. Rev. 188, 2367 (1969).

[52]This strong sensitivity of the two solutions to the value of α_v was pointed out by Garcia in 1971 (see Ref. 7).

[53]R. Winston, private communication.

[54]The most recent experiments reported are those of R. J. Ellis *et al.*, [Nucl. Phys. B39, 77 (1972)], and C. Baltay et al. [Phys. Rev. D 5, 1569 (1972)]. These papers contain references to the earlier experiments.

[55]P. Franzini *et al.*, Phys. Rev. D 6, 2417 (1972).

[56]Note that a second-class coupling in the weak Hamiltonian would lead, via SU(3)-symmetry breaking, to second-class corrections to the first-class form factors. The form factors will also receive $O(\alpha)$ corrections from the radiative corrections to the decays.

[57]$A_\mu^i(x)$ and $V_\mu^j(x)$ are axial-vector and vector currents

normalized to

$$[A_0^i(x), A_\mu^j(0)]_{x_0=0} = i\delta^{(3)}(x) f^{ijk} V_\mu^k(0) + \text{S.T.},$$

where S.T. = Schwinger terms.

[58]S. Weinberg, Phys. Rev. Lett. 18, 507 (1967); S. L. Glashow, H. J. Schnitzer, and S. Weinberg, *ibid.* 19, 139 (1967); T. Das, V. Mathur, and S. Okubo, *ibid.* 18, 761 (1967); H. T. Nieh, *ibid.* 19, 43 (1967).

[59]K. Kawarabayashi and M. Suzuki, Phys. Rev. Lett. 16, 255 (1966); Riazuddin and Fayyazuddin, Phys. Rev. 147, 1071 (1966).

[60]The analysis at this stage closely parallels that of S. Fenster and F. Hussain, Phys. Rev. 169, 1314 (1968).

[61]M. L. Goldberger and S. B. Treiman, Phys. Rev. 110, 1178 (1958).

[62]H. J. Schnitzer and S. Weinberg, Phys. Rev. 164, 1828 (1967).